NATIONAL WATER RESEARCH INSTITUTE

INSTITUT NATIONAL de RECHERCHE sur les EAUX

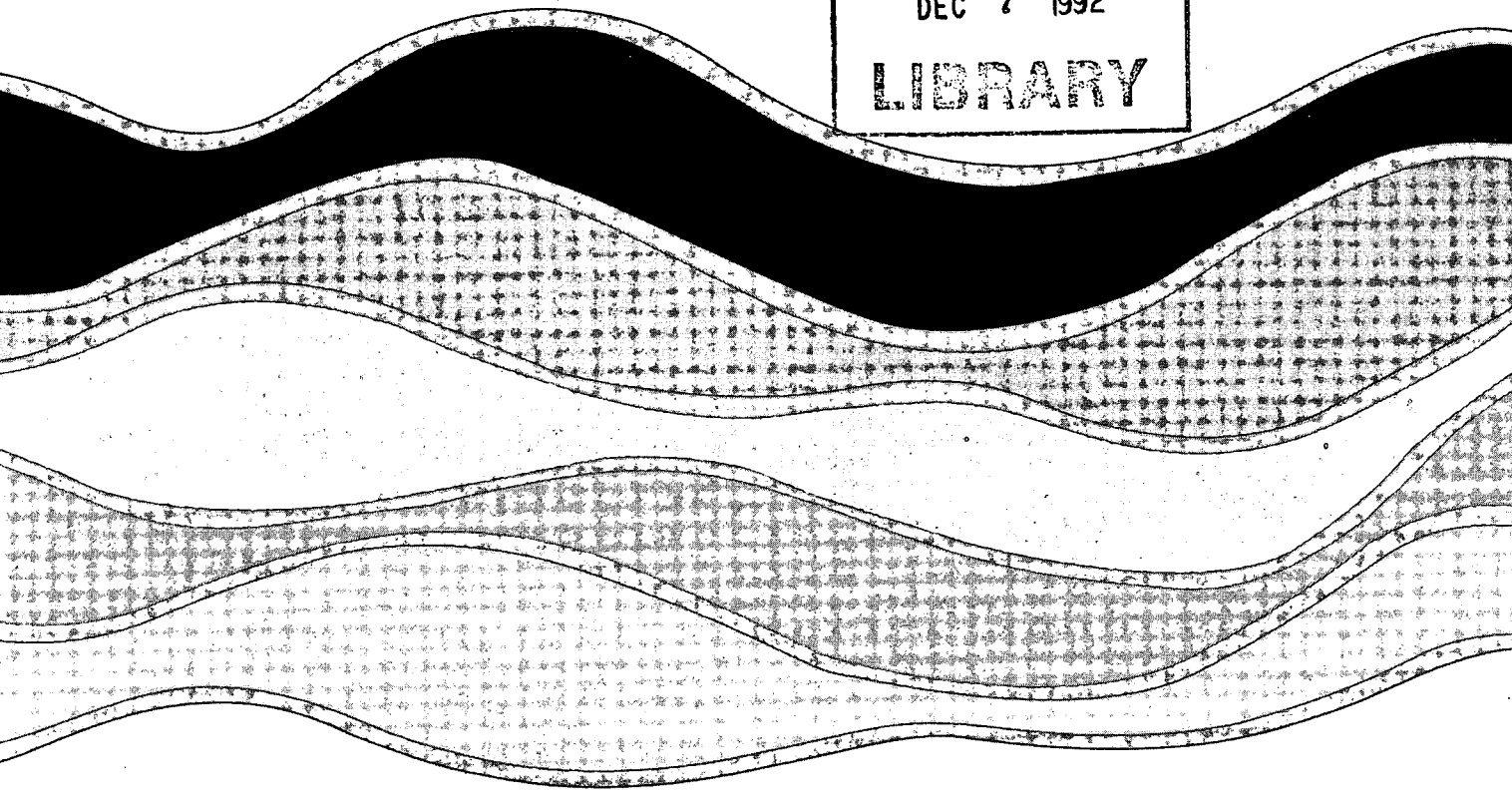

EFFECTS OF NOZZLE AND AIR VENT SIZE ON SEDIMENT SAMPLER PERFORMANCE

P.Engel and *I.G.Droppo*[1]

Research and Applications Branch

National Water Research Institute

Burlington, Ontario L7R 4A6

[1]Rivers Research Branch

National Water Research Institute

Burlington, Ontario L7R 4A6

NWRI Contribution No. 92-06

MANAGEMENT PERSPECTIVE

Accurate measurement of suspended sediment concentration is a fundamentally important requirement in solving environmental problems. The Survey and Information Systems Branch (SISB) of the Ecosystem Science and Evaluation Directorate (ESED), is responsible for the performance of about 500 suspended sediment samplers in a nationwide data collection program. The adjustment and calibration of these samplers requires significant time and resources. A strategy of sampler evaluation and calibration to meet these needs is being developed jointly by the SISB and the Research and Applications Branch (RAB) of the National Water Research Institute (NWRI). The Rivers Research Branch (RRB) of the NWRI conducts intensive surveys in Southern Ontario rivers to examine their sediment and contaminant loading regimes. Improved performance of existing suspended sediment samplers has a high priority. To meet the needs of the SISB and the RRB, an experimental study has been conducted in the towing tank of the Hydraulics Laboratory using one US DH-81 sampler, fitted with four different sized nozzles and five different air exhaust vent sizes. The test results have shown that the performance of samplers is highly dependent on the relative size of nozzle and air vent diameters. Using dimensional analysis, criteria governing the behaviour of the US DH-81 sediment sampler under nozzle control and air vent control were established. This information is important in developing methods to improve sampler performance and to develop a strategy for quality control of sediment samplers. The study was conducted jointly by the RAB and the RRB.

SOMMAIRE À L'INTENTION DE LA DIRECTION

La mesure exacte de la concentration de matières en suspension dans l'eau est un élément fondamental de la résolution des problèmes d'environnement. La Direction des relevés et systèmes d'information, de la Direction générale des sciences et de l'évaluation des écosystèmes, est responsable de la performance d'environ 500 échantillonneurs de matières en suspension qui servent dans un programme national de cueillette de données. L'ajustement et l'étalonnage de ces échantillonneurs exigent du temps et beaucoup de ressources. La Direction des relevés et systèmes d'information et la Direction de la recherche pure et appliquée de l'Institut national de recherche sur les eaux élaborent conjointement une stratégie d'évaluation et d'étalonnage des échantillonneurs en vue de répondre à ces besoins. La Direction de la recherche sur les cours d'eau, INRE, procède à des relevés intensifs des rivières situées dans le sud de l'Ontario afin d'examiner leurs régimes de charge sédimentaire et de contaminants. L'amélioration de la performance des échantillonneurs de matières en suspension est grandement prioritaire. Afin de répondre aux besoins de la Direction des relevés et systèmes d'information et de la Direction de la recherche sur les cours d'eau, on a procédé à des essais sur un échantillonneur US DH-81 dans le bassin à chariot mobile du laboratoire d'hydraulique. Quatre ajutages de calibres différents et cinq orifices d'évacuation d'air de calibres différents ont été testés. Les résultats ont établi que la performance des échantillonneurs dépend fortement de la dimension relative des diamètres de l'ajutage et de l'orifice d'évacuation d'air. À partir d'une analyse dimensionnelle, on a établi les critères du comportement de l'échantillonneur de sédiments US DH-81 selon qu'il fonctionne sous contrôle par l'ajutage ou par l'orifice d'évacuation d'air. Les renseignements obtenus seront très utiles dans l'élaboration de méthodes visant à améliorer la performance de l'échantillonneur et dans le développement d'une stratégie pour le contrôle de qualité des échantillonneurs de sédiments. L'étude a été assurée conjointement par la Direction de la recherche pure et appliquée ainsi que la Direction de la recherche sur les cours d'eau.

ABSTRACT

Using dimensional analysis and experimental datas, it has been shown that the performance of the US DH-81 sampler is highly dependent on the relative size of nozzle and air vent diameters. It is shown that the sampler has a distinct flow control regime which depends primarily on the relative size of the nozzle intake diameter and the air vent diameter. If flow control is at the nozzle, the flow rate into the sampler can be significantly increased by changing certain geometric properties of the nozzles. If flow control is at the air vent, iso-kinetic performance can be achieved by varying the air vent diameter. It is further shown that the *Sampler Performance Coefficient* is strongly dependent on a dimensionless variable designated as the *Sampler Number* which accounts for the viscosity of the water when the sampler operates under nozzle control and viscosity of the air in the sampler when flow control is at the air vent.

RÉSUMÉ

À partir d'une analyse dimensionnelle et de données expérimentales, il a été établi que la performance de l'échantillonneur US DH-81 dépend fortement de la dimension relative des diamètres de l'ajutage et de l'orifice d'évacuation d'air. Il est établi que l'échantillonneur a un régime particulier de contrôle du débit qui dépend avant tout de la dimension relative du diamètre de l'ajutage et du diamètre de l'orifice d'évacuation d'air. Lorsque le contrôle de l'écoulement se fait par l'ajutage, le débit d'eau qui pénètre dans l'échantillonneur peut être considérablement accru par la modification de certaines propriétés géométriques de l'ajutage. Lorsque le contrôle de l'écoulement est assuré par l'orifice d'évacuation d'air, il est possible d'obtenir une performance isocinétique en faisant varier son diamètre. Il est établi en outre que le *Coefficient de performance de l'échantillonneur* est en forte corrélation avec une variable sans dimension qu'on appelle *nombre de l'échantillonneur*, qui permet de tenir compte de la viscosité de l'eau lorsque l'échantillonneur fonctionne sous contrôle par l'ajutage, et qui permet de tenir compte de la viscosité de l'air dans l'échantillonneur lorsque le contrôle de l'écoulement est assuré par l'orifice d'évacuation d'air.

TABLE OF CONTENTS

1. INTRODUCTION

Accurate measurement of suspended solids concentration and distribution is critical in the study of sediment and contaminant transport. A variety of samplers for measuring suspended sediment concentration in rivers have been developed over the last fifty years (U.S.A.C.E. 1941, T.C.P.S.M. 1969, Guy and Norman 1970 and Cashman 1988). However, only two depth integrating type samplers classified by the U.S. Federal Inter-Agency Sedimentation Project as US D-77 and US DH-81 are relevant to the sampling of contaminated sediments because all components exposed to the water sample are of autoclavable plastics. The D-77 sampler was designed to collect large volume samples from streams at near freezing temperatures but can be used under low flow conditions at higher temperatures. The DH-81 sampler is an adaptation of the D-77 and is used for sampling normal flow in small to intermediate sized streams or through the ice, suspended with a wading rod. The D-77 sampler has been found to over-sample the flow rate at low velocities and under-sample the flow rate at higher velocities (Skinner 1979). A similar behaviour has been observed with the DH-81 sampler by Engel and Droppo (1990).

Suspended sediment samplers are operated on the premise that the velocity of flow through the nozzle is equal to the velocity of the stream flow surrounding the nozzle. This condition is known as iso-kinetic sampling. For sediment sampling quality control, nozzle velocity V_n and the stream flow velocity V_s, are expressed as a ratio given by

$$K = \frac{V_n}{V_s} \tag{1}$$

where K is the *Sampler Performance Coefficient.* For iso-kinetic conditions, $K = 1$ and it is assumed that the flow entering through the nozzle contains the same sediment-water mixture as the stream flow being sampled. When $K > 1$ the sampler will under-sample the suspended sediment concentration, whereas when $K < 1$ the sampler will over-sample (Beverage and Futrell 1986). These conditions are not important when the

sediment concentration is uniform over the depth of flow. However, most frequently one encounters a concentration gradient, with the concentration increasing with depth from the free surface. Tests by Engel and Droppo (1990) on a DH-81 Sampler, equipped with a 7.94 mm (5/16") nozzle, in a towing tank have shown that the value of K depends on the size of the air vent diameter. In this report, the performance of the DH-81 sampler is examined when both the nozzle and air vent diameter are varied. The results will provide the necessary information required to establish guide lines for the calibration and operation of suspended sediment samplers.

2.0 PRELIMINARY CONSIDERATIONS

2.1 Factors Affecting Control of Flow Into the Sampler

The relative importance of the nozzle and the air vent in establishing flow control depends on the energy losses each imposes on the flow. It has been shown by Engel (1991b) that, if the losses at the air vent and the losses at the nozzle are expressed as E_D and E_n respectively, one may write

$$E_D = \left(K_D + 1\right)\left(\frac{d}{D}\right)^4 \tag{2}$$

and

$$E_n = \left\{K_c + K_e + K_s\left(\frac{d}{d_o}\right)^4 + f\left(\frac{L_s}{d}\right)\right\} \tag{3}$$

where K_D = the coefficient of energy loss due to the air flow contraction at the air vent, K_c = the coefficient of energy loss due to the flow contraction at the nozzle entrance, K_e = the coefficient of energy loss due to the gradual expansion of the nozzle flow passage, K_s = the coefficient of energy loss due to the sudden expansion from the nozzle outlet into the sampler cavity, d_o = the internal diameter at the nozzle outlet, f = the Darcy-Weisbach friction factor for the nozzle and L_s = the length of the flow

passage of the nozzle. The relative importance of E_D and E_n can be expressed as

$$N_c = \frac{(K_D + 1)\left(\frac{d}{D}\right)^4}{\left\{K_c + K_e + K_s\left(\frac{d}{d_o}\right)^4 + \left(f\frac{L_s}{d}\right)\right\}} \tag{4}$$

where N_c may be designated as the *Flow Control Number* for the sampler. When $N_c > 1$, losses at the air vent are larger so that the air vent control is dominant. When $N_c < 1$, losses at the nozzle are larger so that the flow into the sampler is controlled primarly by the nozzle. When $N_c = 1$, the sampler is at the point of transition between nozzle and vent control.

The flow control regime can be altered by changing E_D and E_n. This means that for a given sampler operating under nozzle control, the flow control can be shifted towards vent control depending on the amount that E_n can be decreased and/or E_D can be increased. Examination of E_n shows that opportunities for changes are limited. The friction factor f depends on the nozzle Reynolds number and the nozzle length L_s is small and virtually fixed for each nozzle. Therefore, limited change in the dimensionless variable $f\frac{L_s}{d}$ can be made by changing the nozzle diameter d. Values of K_c are affected by the geometry at the nozzle entrance such as the radius of curvature of the entrance lip, the external angle of taper of the nozzle nose, the thickness of the nozzle wall at the entrance and the length of the nozzle protruding from the sampler nose. There are significant differences in these geometrical characteristics for the four nozzles tested and can be expected to account for some of the difference in their performance. However, these variables cannot be changed sufficiently to effect significant changes in the energy loss coefficients for any one nozzle. Tests results from Engel (1991a) have shown that some increase in nozzle velocity can be obtained by increasing the nozzle outlet diameter d_o. This means that for a given nozzle diameter d, the variable $\frac{d}{d_o}$ in equation (4) is reduced, resulting in a reduction in the value of E_n, which in turn increases the *Flow Control Number* N_c and moves the sampler flow regime in the direction of vent control. This procedure is only useful when values of K in equation (1) are only slightly below the iso-kinetic value of 1.0. A prudent increase in d_o will then increase the value of K

to the desired value of 1.0.

Values of N_c can be changed more effectively by changing E_D. Similar to the case of entrance loss coefficient for nozzles K_c, changes in K_D will have only limited effect. However, significant changes in the sampler performance can be obtained by changing $\frac{D}{d}$. Equation (4) shows that decreasing $\frac{D}{d}$ increases N_c by increasing the energy losses at the air vent and thus moves the flow regime in the sampler further towards vent control.

It can be seen from equation (4) that the performance of the sampler depends not only on the ratio $\frac{D}{d}$ but on the geometric properties of the nozzles as well. Therefore, for a given value of $\frac{D}{d}$, one can expect a different value of N_c for each of the four different sizes of nozzles available. Experiments were conducted to determine the performance of the US DH-81 sediment sampler with each of these nozzles.

3.0 EXPERIMENTAL EQUIPMENT AND PROCEDURE

3.1 Towing Tank

The towing tank used to test the DH-81 sampler is 122 m long by 5 m wide and is constructed of reinforced concrete founded on piles. The full depth of the tank is 3 metres, of which 1.5 metres are below ground level. Normally the water depth is maintained at 2.7 metres. Concrete was chosen for its stability and to reduce possible vibrations and convection currents.

At one end of the tank is an overflow weir. Waves arising from towed objects and their suspensions are washed over the crest, thereby reducing wave reflections. Parallel to the sides of the tank perforated beaches serve to dampen lateral surface wave disturbances.

3.2 Towing Carriage

The carriage is 3 metres long, 5 metres wide, weighs 6 tonnes and travels on four precision machined steel wheels. The carriage is operated in three overlapping velocity ranges:

0.005 m/s - 0.06 m/s

0.05 m/s - 0.60 m/s

0.50 m/s - 6.00 m/s

The maximum velocity of 6.00 m/s can be maintained for 12 seconds. Tachometer generators connected to the drive shafts emit a voltage signal proportional to the velocity of the carriage. A feedback control system uses these signals as input to maintain constant velocity during tests.

The average velocity data for the towing carriage is obtained by recording the voltage pulses emitted from a measuring wheel. This wheel is attached to the frame of the towing carriage and travels on one of the towing tank rails, emitting a pulse for each millimeter of travel. The pulses and measured time are collected and processed to produce an average towing velocity with a micro computer data acquisition system. Analysis of the towing velocity variability by Engel (1989), showed that for velocities between 0.2 m/s and 3.00 m/s, the error in the mean velocity was less than ±0.15% at the 99 % confidence level. Occasionally, these tolerances are exceeded as a result of irregular occurrences such as "spikes" in the data transmission system of the towing carriage. Tests with such anomalies are recognized by the computer and are automatically aborted.

3.3 The US DH-81 Sampler and Appurtenances

The sampler consists of a DH-81 adapter, a US D-77 cap, four sampling nozzles with 3.18 mm (1/8"), 4.76 mm (3/16"), 6.35 mm (1/4") and 7.94 mm (5/16") inside

diameters, a plastic "mason-jar" threaded bottle with 3 litre capacity and a wading rod. The components of the sampler are given in Figure 1 and the assembled sampler is given in Figure 2.

The US DH-81 sampler is designed to sample low velocity rivers by wading or by sampling through the ice cover (Cashman 1988). The sampler allows for large sample volumes (2700 ml), providing the large samples required for sedimentological analysis. When the sampler is lowered into the flow, air is expelled through a 3.0 mm diameter air vent at the top of the sampler cap shown schematically in Figure 3. A small "horn" protruding from the sampler cap just ahead of the air vent presents a "bluff" body to the flow resulting in a small, negative pressure pocket immediately behind it. This creates a "suction" effect which effectively reduces the energy drop through the air vent (Engel 1991b). Finally, the air vent outlet is located about 2 cm above the centre-line of the nozzle flow passage. This creates a small, constant, positive, hydro-static pressure which prevents water from entering through the air vent.

3.4 Effect of Flow Depth

The DH-81 sampler is open to the outside environment during normal depth integrated sampling. As a result, the air volume inside the samplers is subject to the effect of pressure changes as the sampler is lowered and raised through the flow. Initially, at the surface, the internal cavity of the sampler is at atmospheric pressure because the sampler is open to the air through the nozzle and the air vent. As the sampler is submerged and travels toward the stream bed, the pressure inside the sampler increases in proportion to the flow depth. The increase in static pressure compresses the volume of air in the sampler and this causes an inflow of water through the nozzle in excess of that expected due to the net head (ℓ + velocity head; where ℓ is the static head at the nozzle equal to the difference in elevation of the centre-line of the nozzle and the air vent) alone. During the present tests this problem was minimized by holding the test

sampler fixed at the minimum possible depth of of 0.2 m.

3.5 Test Procedure

The purpose of a suspended sediment sampler is to obtain a sample that is representative of the water-sediment mixture moving in the vicinity of the sampler. During sampling, a volume of the water-sediment mixture is collected in the sampler over a measured interval of time. From the measured volume and time, the flow rate into the sampler is then determined. The velocity of the flow through the nozzle is computed by dividing the flow rate by the cross-sectional area of the nozzle intake. The sediment flux is the product of the sediment concentration of the collected sample and the nozzle velocity.

For a given nozzle, the volume of water that can enter the sampler bottle in a given period of time, should depend among other things, on the the physical properties of the nozzle and the air vent. In order to determine the effect of the vent size on the sampling rate, tests were conducted for towing velocities of 0.2 m/s, 0.4 m/s, 0.6 m/s, 0.8 m/s and 1.0 m/s with air vent diameters of 1.0 mm, 1.5 mm, 2.0 mm, 2.5 mm and 3.0 mm. The sampler used by Engel and Droppo (1990) was used. To vary the size of the air vent this sampler had been modified by drilling out the exhaust vent and tapping it to receive a 6.4 mm (1/4") Allen key plug. Five such plugs were prepared, each with a hole drilled concentric with its longitudinal axis, to provide the new vent hole of the desired size. For each case the Allen key plug was screwed into place so that the bottom of the plug was flush with the crown of the existing vent tunnel leading to the vent (Figure 3). To determine the effect of nozzle size, four standard nozzles having intake diameters of 3.18 mm (1/8"), 4.76 mm (3/16"), 6.35 mm (1/4") and 7.94 mm (5/16") were used.

Each series of runs for a given nozzle size was considered a test. At the

beginning of the test, the chosen nozzle was inserted into the sampler nose, the first of five air vent plugs was screwed into the sampler cap and the sampler assembled. Once the sampler was prepared, the towing carriage was set into motion. When the carriage had reached its pre-set velocity, the sampler was submerged and held at 0.2 m below the surface of the water for a set period of time. Care was taken that the bottle was never more than 2/3 full to ensure that there was no interference in the air flow through the vent due to over-filling. When the set period of sampling time had expired the sampler was removed from the water and the volume of water determined with a 1000 ml graduated cylinder. The velocity of flow through the sampler nozzle was then computed from the equation

$$V_n = \frac{1.273 V_w}{d^2 t_s} \tag{5}$$

and the inflow of water into the sampler was determined as

$$Q_s = \frac{V_w}{t_s} \tag{6}$$

where d = the diameter of the nozzle inlet, V_w = the volume of water collected, t_s = the time over which the sampler was submerged and Q_s = the rate of flow of water into the sampler.

For each of the five air vent sizes, two runs were conducted at each of the selected towing velocities and their average computed. The tests for the remaining three nozzles were conducted in the same way. In all, four tests, each consisting of 25 runs, were completed for a total of 100 runs. The data are given in Tables 1 to 4.

4.0 DATA ANALYSIS

4.1 Flow into the Sampler

Data from Table 1 to 4 were plotted as Q_s vs. the towing velocity V_c with D as a parameter in Figure 4 for each of the four nozzles tested. Smooth curves were

drawn through the data points to facilitate the analysis. The curves clearly show the effect of the nozzles. In all cases the inflow increased as the towing velocity increased with the rate of change increasing as the nozzle diameter d increased. The curves also clearly show the effect of nozzle size on the flow rate into the sampler. For a given towing velocity V_c, values of Q_s increased as d increased.

The curves in Figure 4 also show quite clearly the effect of the air vent diameter for a given flow condition. The effect of D is very much dependent on the size of the nozzles. When $d = 3.18$ mm, the inflow is affected by the air vent only for $D < 1.5$ mm. Once the air vent has reached a diameter of 1.5 mm, any further increases in D has no significant effect on the rate of flow into the sampler through the nozzle. This means that when $D \geq 1.5$ mm, the sampler operates under nozzle control. A similar observation can be made for the 4.76 mm nozzle. Once again the air vent affects the flow into the sampler only for values of $D < 1.5$ mm. For values of $D \geq 1.5$ mm, the effect of the air vent is negligible and the sampler again operates under nozzle control. The effect of the air vent becomes increasingly important as the size of the nozzles increase. This is because, for a given towing velocity, the value of Q_s increases, requiring an equivalent volume of air to be expelled. As a result, an increasingly larger value of D is required to allow uninhibited release of air and thus permit the control of the flow to be at the nozzle. When the nozzle diameter has reached a value of 6.35 mm, the curves in Figure 4 show that the air vent affects the inflow for all values of D, although the effect decreases as D increases. Finally, when $d = 7.94$ mm, the effect of the air vent is most pronounced. There is a significant effect on the inflow even when the air vent diameter is at the maximum tested value of 3.0 mm. Therefore, when the nozzle diameter is 7.94 mm, the sampler operates primarily under air vent control.

The effect of D, as one would expect, also increases as the towing velocity increases and the magnitude of this effect depends on the nozzle diameter d. This is quite evident in Figure 5 in which Q_s is plotted as a function of d with D as a

parameter for given values of V_c. Once again smooth curves were fitted to the data points to facilitate the analysis. The curves clearly show the increase in Q_s as d increases for each value of $D > 1.0$ mm and that this increase depends on the towing velocity V_c. When $D = 1.0$ mm, Q_s initially increases as d increases and then exhibits a slight decrease, with the magnitude of this change being greatest at the highest value of V_c. This behaviour demonstrates that the flow control at the air vent increases as the size of the nozzle and thus the capacity for inflow increases, because of the increased restriction on the escaping air flow. The pattern of the curves clearly shows the conditions for which the flow is controlled by the nozzle and the air vent. For towing velocities up to 0.80 m/s and values of $D > 1.0$ mm, the flow is controlled by the nozzles as long as their diameter is less than about 5.0 mm. For the 7.94 mm nozzle the flow will be affected by the air vent for all tested values up to $D = 3.0$ mm.

4.2 Nozzle Velocity Versus Towing Velocity

The flow into the sampler gives a good indication of the factors governing the performance of the sampler. However, the control of the flow into the sampler must be such that iso-kinetic conditions prevail. Therefore, it is important to determine for what conditions the flow velocities through the nozzle are equal to the velocities at which the sampler is towed. In order to examine the sampler performance, the data in Tables 1 to 4 were plotted as V_n vs. V_c with the air vent diameter as a parameter for each of the four sizes of nozzles in Figure 6. Smooth curves were again drawn through the data points to facilitate the analysis. The plots clearly show the effect of the air vent diameter and the nozzle size. The relative effects are clearly revealed by comparison with the 45^0 iso-kinetic line shown in each of the plots. In all cases, the nozzle velocity increases as the carriage velocity increases with the rate of change being greatest for the smallest nozzle size for all air vent diameters and the rate of change decreasing as the diameter of the nozzles increases. Generally, values of the nozzle velocities are highest for the 3.18 mm nozzle and this difference, compared to the larger nozzles, is

most pronounced at the smaller values of the air vent diameter. As the diameter of the nozzles increases, the range in values of nozzle velocities increases for the same values of $1.0 \leq D \leq 3.0$. It is also quite clear from Figure 6 that the most favourable conditions are obtained when the 4.76 mm (3/16") nozzle is used. In this case, the data for $1.5 \leq D \leq 3.0$ plot very close to the iso-kinetic line for values of $V_c \geq 0.50$ m/s. Similar results are obtained for the 6.35 mm (1/4") nozzle for $2.5 \leq D \leq 3.0$ and for the 7.94 mm (5/16") nozzle when the air vent diameter is 2.5 mm. It seems quite clear that nozzle diameter is a significant variable governing the performance of the DH-81 sampler.

The effect of the nozzle diameter can be seen directly by plotting V_n vs. V_c with nozzle diameter d as a parameter for each value of the air vent diameter D. Such plots are given in Figure 7. The curves again show the undesirable results when $D = 1.0$ mm. As the air vent diameter increases, values of nozzle velocity increase reaching values closer to the iso-kinetic line as D increases. When $D = 2.0$ mm, data for the three larger nozzles can be described by a single curve crossing the iso-kinetic line when $V_c = 0.60$ m/s. For $V_c \geq 0.60$ m/s, values of the nozzle velocity are too large whereas for $V_c \leq 0.60$ m/s, values of the nozzle velocity are too small with the decrement increasing as the carriage velocity increases. When $D = 2.5$ mm, the curves for the 4.76 mm and 7.94 mm nozzles are virtually coincident, indicating iso-kinetic performance for $V_c \geq 0.80$ m/s. The curve for the 6.35 mm nozzle gives nozzle velocities slightly lower and falling below the iso-kinetic line for carriage velocities greater than 0.60 m/s. Finally, when $D = 3.0$ mm, the curves for 4.76 mm and 6.35 mm nozzles are virtually coincident giving near iso-kinetic results for carriage velocities greater than 0.80 m/s, whereas the curve for the 7.94 mm nozzle gives values of V_n which are significantly above the iso-kinetic line for all values of V_c.

Further examination of the curves in Figure 7 shows that there is a gradual shifting of relative position of the curves for different values of air vent diameter for

$1.5 \leq D \leq 3.0$. This behaviour appears to be indicative of the relative importance of the nozzles and air vent depending on their respective size and the external flow velocity.

4.3 Nozzle Velocity Versus Nozzle Diameter

The relative importance of nozzle and air vent diameter can be observed by plotting the data from Tables 1 to 4 as V_n vs. d with V_c as a parameter for given values of D. Such plots are given in Figure 8 with smooth curves again fitted to the data to facilitate the analysis. For values of D equal to 1.0 mm and 1.5 mm, V_n decreases as d increases with the rate of change increasing as values of V_c increase. The rate of change in V_n as d increases is less for the case of $D = 1.5$ mm than it is when $D = 1.0$ mm. As values of D increase above 1.5 mm, the change in V_n with d becomes increasingly more pronounced. When $D = 2.0$ mm, V_n initially decreases as d increases for each value of V_c, reaching a minimum value and gradually increasing with further increase in d. A similar but more distinctive behaviour is observed at values of $D = 2.5$ mm and 3.0 mm. The increase in V_n indicates that the flow into the sampler is controlled by the air vent and may also be somewhat dependent on the overall geometry of the nozzle. The increase in the air vent diameter creates the freedom for increased flow rate through the sampler whereas changes in the nozzle geometry may also result in small changes in energy losses as shown in equation (4).

The effect of the air vent diameter for a given carriage velocity can be revealed directly by plotting the data given in Tables 1 to 4 as V_n vs. d with D as a parameter for each value of the carriage velocity V_c. These data are plotted in Figure 9 and once again smooth curves have been fitted to the data to facilitate the analysis. The curves once again show the change in nozzle velocity as a function of nozzle diameter seen in Figure 8. The relative positions of the curves give a clear indication of the relative importance of the nozzle size and air vent diameter. For the case of $V_c = 0.20$ m/s, curves are given only for $D \geq 2.0$ mm because of the erratic response of the sampler

at these low velocities for the smaller air vent diameters. When $V_c \geq 0.40$ m/s, the curves clearly show the dominance of the air vent control for $D \leq 2.0$ mm and its dependence on the carriage velocity V_c. For all values of d the greatest change in V_n occurs when D is changed from 1.0 mm to 1.5 mm. This sensitivity in vent control decreases as carriage velocity increases and the nozzle diameter increases. As values of D increase from 1.5 mm to 3.0 mm the effect of the air vent depends both on nozzle size and carriage velocity. When $V_c = 0.20$ m/s, some sensitivity to changes in D can be observed for values of $d \leq 5$ mm and values of $d \geq 5$ mm. In the vicinity of $d = 5$ mm, changing the air vent diameter seems to have no effect on the nozzle velocity. When the carriage velocity is increased to 0.40 m/s, effects of changing the air vent diameter are insignificant for nozzles smaller than 5 mm and air vent diameters greater than 2.5 mm. For values of $d \geq 5$ mm, the flow rate through the nozzle is affected by changing D. Examination of the curves for $V_c = .60$ m/s, shows that the effect of changing D when $D \geq 2.0$ mm, is virtually negligible for $d = 3$ mm. The effect of D increases slowly as d increases. When $V_c = 0.80$ m/s, the effect of changing D is virtually insignificant for $D \geq 2.0$ mm and $d \leq 4.5$ mm. For values of $d > 4.5$ mm, the effect of D increases as d increases. Finally, when $V_c = 1.00$ m/s, the effect of D has become much smaller for values of $D \leq 1.5$ mm when $d < 5$ mm. The effect of D is negligible when $D \geq 2.0$ mm in this range. The effect of D again increases as d increases.

The effect of the air vent diameter as indicated by the curves in Figure 9, provides some information on the complexity of the performance characteristics of a sediment sampler. When the flow rate through the nozzle is affected by changing the air vent diameter, the sampler is operating under air vent control. Alternatively, when changing the air vent diameter has no significant effect on the nozzle velocity, the sampler can be said to operate under nozzle control. The results suggest that, for standard samplers, nozzle control is restricted to nozzles of small diameter to ensure that the air vent is of sufficient size to permit free voiding of air from the sampler. Knowledge of the flow control regime of a sampler is important for their calibration to

ensure that sampling is done under iso-kinetic conditions.

4.4 Flow Control

It has been shown that the flow control regime of a given sampler depends largely on the nozzle size but also on geometric characteristics of the nozzles. Therefore, the value of $\left(\frac{D}{d}\right)$ at which control changes from the nozzle to the air vent should be unique for a nozzle with particular properties. Using equation (4) this value can be expressed as

$$\left(\frac{D}{d}\right)_c = \left\{\frac{(K_D+1)}{\left[K_c+K_e+K_s\left(\frac{d}{d_o}\right)^4+f\left(\frac{L_s}{d}\right)\right]}\right\}^{\frac{1}{4}} \tag{7}$$

where $\left(\frac{D}{d}\right)_c$ is the value of $\frac{D}{d}$ at which flow control changes from the nozzle to the air vent. Equation (7) shows that the value $\left(\frac{D}{d}\right)_c$ is not very sensitive to changes in K_D. This means that changes to the geometry of the intake of the air vent outlet will not bring about significant improvement in the performance of the sampler.

The energy loss coefficients in equation (7) are not known for the case of flow through sampler nozzles. A more direct way to define the flow regime of a sampler with a particular nozzle, is through dimensional analysis, considering separately the flow through the nozzle and the air vent.

In general, the flow through a particular nozzle can be expressed as

$$f_n(V_c, Q_s, d, \nu_w, \rho_w) = 0 \tag{8}$$

where f_n is a function describing the flow through the nozzle, Q_s = the flow rate of water into the sampler, ν_w = the kinematic viscosity of water, ρ_w = the density of water and all other variables have already been defined. Using dimensional analysis one obtains

$$\frac{Q_s}{d^2 V_c} = f_{n1}\left(\frac{Q_s}{d\nu_w}\right) \tag{9}$$

where f_{n1} = a dimensionless function. Similarly, the general functional relationship for the air flow at the vent can be expressed as

$$f_a(V_c, Q_s, D, \nu_a, \rho_a) = 0 \tag{10}$$

where D = the diameter of the air vent, ν_a = the kinematic viscosity of the air inside the sampler cavity, ρ_a = the density of the air inside the sampler cavity and all other variables have already been defined. Once again, using dimensional analysis yields

$$\frac{Q_s}{D^2 V_c} = f_{a1}\left(\frac{Q_s}{D\nu_a}\right) \tag{11}$$

where f_{a1} = a dimensionless function. The point of flow control transition from nozzle control to vent control can be obtained by combining equation (9) and (11) to give

$$F\left(\frac{D}{d}, \frac{Q_s}{d\nu_w}, \frac{Q_s}{D\nu_a}\right) = 0 \tag{12}$$

where F represents another dimensionless function. The condition of $N_c = 1$ can be obtained by defining the maximum value of $\frac{D}{d}$ for which vent control is in effect. Therefore, after some further simplifications, equation (12) can be expressed in the more convenient but equivalent form

$$F_t\left\{\left(\frac{D}{d}\right)_c, \frac{Q_s}{d\nu_w}, \frac{\nu_a}{\nu_w}\right\} = 0 \tag{13}$$

where F_t is a function which represents the flow in the sampler at the point where flow control changes from nozzle control to vent control and $\left(\frac{D}{d}\right)_c$ is the maximum value of $\frac{D}{d}$ at which vent control exists. Equation (13) can be rearranged to the form

$$\left(\frac{D}{d}\right)_c = F_t\left\{\frac{Q_c}{d\nu_w}, \frac{\nu_a}{\nu_w}\right\} \tag{14}$$

The curves in Figure 4 show that for the 3.18 mm nozzle, the maximum value of D for which air vent control exists is 1.5 mm and that this is independent of the flow rate Q_s and the towing velocity V_c. This means that for the same nozzle, values of $\left(\frac{D}{d}\right)_c$ is independent of the Reynolds number $\frac{Q_s}{d\nu_w}$. The same thing is true for the 4.76 mm

nozzle. For the two larger sized nozzles, the sampler operates under vent control in all cases and the question of control transition does not arise. Having determined that the Reynolds number is not important for determining the maximum value of $\frac{D}{d}$, equation (14) can be further simplified to give

$$\left(\frac{D}{d}\right)_c = \Phi_t\left\{\frac{\nu_a}{\nu_w}\right\} \tag{15}$$

where Φ_t denotes another dimensionless function. Although the four types of nozzles tested have different geometric properties, one can expect that the greatest effect on the flow control is exerted by the diameter d. Therefore, values of $\left(\frac{D}{d}\right)_c$ are plotted for each value of d in Figure 10 for the value of $\frac{\nu_a}{\nu_w} \approx 15$ maintained during the tests. Figure 10 shows regions delineated by values of $\left(\frac{D}{d}\right)_c$ and $\left(\frac{D}{d}\right)_{min}$. The latter ratio denotes the value for the smallest functional vent diameter. For the two smaller nozzles there are regions of nozzle control and vent control. For a given vent size, if the nozzle diameter is such that $\frac{D}{d}$ falls into the region of nozzle control, then the performance of the sampler can be changed by making changes to the nozzle. Alternatively, if the sampler operates under vent control, the sampler's performance can be changed by changing the air vent size. For the two larger nozzles the sampler was found to be operating entirely under vent control for all values of $\frac{D}{d}$. Vent control is more effective and is thus very useful for the design of a completely iso-kinetic sediment sampler as reported by Engel and Droppo (1990). Figure 10 may be considered to be a *Flow Control Diagram* for the US DH-81 sediment sampler when $\frac{\nu_a}{\nu_w} \approx 15$.

4.5 Sampler Performance Under Nozzle Control

It has been shown that a given sediment sampler operates under the combined influence of the nozzle and the air vent, with the flow control of the sampler depending largely on the magnitude of the diameter ratio $\frac{D}{d}$ and the overall geometric features of the nozzle. As a result, for a given nozzle, the flow velocity in the nozzle can be

expressed in the general functional form

$$V_n = F_n(V_c, d, D, \rho_w, \nu_w) \tag{16}$$

where F_n denotes a function and all other variables have already been defined. Using dimensional analysis, one obtains

$$\frac{V_n}{V_c} = F_{n1}\left(\frac{V_c d}{\nu_w}, \frac{D}{d}\right) \tag{17}$$

where F_{n1} denotes a dimensionless function and after remembering that the *Sampler Performance Coefficient* is given as $K = \frac{V_n}{V_c}$, then from equations (17), one obtains

$$K_n = F_{n2}\left(\frac{V_c d}{\nu_w}, \frac{D}{d}\right) \tag{18}$$

where F_{n2} denotes another function, K_n is the *Sampler Performance Coefficient* and $\frac{V_c d}{\nu_w}$ is the *Sampler Number* when the sampler operates under nozzle control.

The test data were plotted as K_n versus $\frac{V_c d}{\nu_w}$ with $\frac{D}{d}$ as a parameter in Figures 11 and 12 for the case of nozzle control. The plotted points were connected by straight lines to facilitate the analysis. The plots show that values of K_n are dependent on the *Sampler Number* and that this is largely a function of $\frac{D}{d}$. Values of K_n initially decrease as *Sampler Number* increases until a particular value of the latter has been reached. Thereafter, values of K_n change only slightly with further increase in the *Sampler Number*. When the 3.18 mm nozzle is used, values of K_n are always larger and the rate of decrease in K_n, as $\frac{V_c d}{\nu_w}$ increases, is greater than that obtained with the 4.76 mm nozzle. In addition, values of K_n are always greater than 1.0 and are strongly dependent on $\frac{D}{d}$. This dependence on $\frac{D}{d}$ is greatest for the smaller values of the *Sampler Number* and decreases as the latter increases. When $\frac{V_c d}{\nu_w} \approx 2200$, the effect of $\frac{D}{d}$ becomes negligible for $\frac{D}{d} \geq 0.630$. In the case of the 4.16 mm nozzle, for values of $\frac{V_c d}{\nu_w} \geq 2550$, values of $K_n = 1.0 \pm 0.10$ and results improve slightly as $\frac{D}{d}$ increases. The best results are obtained with the 4.76 mm nozzle when the air vent diameter is larger than about 2.5 mm.

The effect of the nozzle geometry can be observed by comparing Figures 11 and 12 for the case of $\frac{D}{d} = 0.630$ which is common to both nozzles. Values of K_n for the 3.18 mm nozzle are significantly larger than those obtained with the 4.76 mm nozzle for similar values of the *Sampler Number*. This suggests that performance can be improved by changing the geometry of nozzles when samplers operate under nozzle control, thereby bringing values of K_n closer to the desired value of 1.0. In their present configurations the 4.16 mm nozzle gives results much superior to those obtained with the 3.18 mm nozzle. Indeed, the results clearly show that iso-kinetic operation of the DH-81 sampler is not possible when the 3.18 mm nozzle is used.

4.6 Sampler Performance Under Vent Control

When the sampler operates under the control of the air vent, then for a given nozzle, the velocity of flow through the nozzle can be expressed by the general functional relationship

$$V_n = F_v(V_c, d, D, \rho_a, \nu_a) \tag{19}$$

where F_v and all other variables have already been defined. Using dimensional analysis, one obtains

$$\frac{V_n}{V_c} = F_{v1}\left(\frac{V_c d}{\nu_a}, \frac{D}{d}\right) \tag{20}$$

where F_{v1} denotes a dimensionless function. Once again remembering that the *Sampler Performance Coefficient* is given as $K = \frac{V_n}{V_c}$, one obtains

$$K_v = F_{v2}\left(\frac{V_c d}{\nu_a}, \frac{D}{d}\right) \tag{21}$$

where F_{v2} denotes another function, K_v is the *Sampler Performance Coefficient* and $\frac{V_c d}{\nu_a}$ is the *Sampler Number* when the sampler operates under vent control.

The test data were plotted as K_v versus $\frac{V_c d}{\nu_a}$ with $\frac{D}{d}$ as a parameter in Figures 13 and 14 for the case of vent control. The plotted points were again connected by straight lines to facilitate the analysis. The plots clearly show that values of K_v increase

as values of $\frac{D}{d}$ increase for all values of the *Sampler Number* with the rate of increase in K_v diminishing as $\frac{D}{d}$ becomes larger. The dependence of K_v on $\frac{D}{d}$ shows that the performance of the sampler can be adjusted by changing the air vent diameter as long as the sampler is operating under air vent control.

The plots in Figure 13 and 14 also show, that for a given value of $\frac{D}{d}$, K_v varies significantly with the *Sampler Number*. Over the range of test results, values of K_v decrease as $\frac{V_c d}{\nu_a}$ increase with the rate of change decreasing as the *Sampler Number* increases. The plots suggest that for each value of $\frac{D}{d}$, there is a critical value of $\frac{V_c d}{\nu_a}$ at which K_v becomes independent of the *Sampler Number*. For the 6.35 mm nozzle, when $\frac{D}{d} = 0.157$, the critical value is $\frac{V_c d}{\nu_a} \approx 340$. The critical value of $\frac{V_c d}{\nu_a}$ increases as $\frac{D}{d}$ increases. When the 7.94 mm nozzle is used, the critical value of the *Sampler Number* is about 420 when $\frac{D}{d} = 0.126$. Once again the critical value of $\frac{V_c d}{\nu_a}$ increases slightly as $\frac{D}{d}$ increases. For best results the US DH-81 sampler should be used with an air vent diameter of 2.0 mm or 2.5 mm when the 6.35 mm and 7.94 mm nozzles are used.

Clearly, it is not possible to have an air vent of a particular diameter for all flow velocities. At best, one could consider each vent diameter to be applicable over a certain range of flow velocity with the extent of each velocity range depending on the sampling accuracy required. However, although using different air vent diameters provides considerable improvement, it is obvious that the use of different discrete air vent sizes is not a fully satisfactory solution. A viable alternative is to use a variable vent control. Engel and Droppo (1990) found that the performance of a US DH-81 sampler with a 7.94 mm nozzle could be controlled with a high degree of repeatability by using a crude air vent valve. It can be seen from Figures 13 and 14 that a vent control valve would operate better with the 7.94 mm nozzle than with the 6.35 mm nozzle. This means that for nozzles of the same geometric properties the valve should be such that values of $\frac{D}{d}$ are small.

Further examination of Figures 13 and 14 shows that there is some influence of nozzle geometry. Comparison of the plots for the common case of $\frac{D}{d} = 0.315$ shows that values of K_v for the 7.94 mm nozzle are slightly larger than those obtained with the 6.35 mm nozzle. The reason for this can be explained with the aid of equation (4) which states that the flow regime of the sampler depends on the *Flow Control Number* N_c. When $N_c > 1$, the sampler operates under vent control. As N_c increases the effect of the nozzles decreases. The plots in Figures 13 and 14 show that the effect of the nozzle becomes increasingly important as the diameter of the nozzles becomes smaller. In other words, a reduction in the size of the nozzle, for a given vent size, means a reduction in the rate of change of water volume inside the sampler resulting in a lower air escape velocity at the vent thereby reducing the resistance losses and the value of N_c.

5.0 CONCLUSIONS

Tests, conducted in a towing tank to determine the effect of different nozzles and air vent diameters on the sampling performance of the US DH-81 suspended sediment sampler, have led to the following conclusions:

When the flow rate through the nozzle is affected by changing the air vent diameter, the sampler is operating under air vent control. Alternatively, when changing the air vent diameter has no significant effect on the nozzle velocity, the sampler can be said to operate under nozzle control. The results suggest that, for standard samplers, nozzle control is restricted to nozzles of small diameter.

When the 3.18 mm and the 4.76 mm nozzles were used, the US DH-81 sampler operated under nozzle control for $D \geq 1.5$ mm. When the 6.35 mm and the 7.94 mm nozzles were used, the sampler operated under air vent control for all values of air vent

diameter $D \leq 3.0$ mm.

The sampler flow control can be expressed by a *Flow Control Number* N_c. Theoretically, when $N_c > 1$, the sampler operates under vent control. When $N_c < 1$, the sampler operates under nozzle control. Results showed that the performance of the US DH-81 sampler was influenced by the geometric properties of the nozzles even when operating under vent control. This implies that standard samplers are operating close to values of $N_c = 1$.

Changes in flow control or sampler performance are most effectively obtained by changing the nozzle diameter and/or the air vent diameter. Sampler performance is most sensitive to changes in $\frac{D}{d}$ when large diameter nozzles are used. Under such conditions the sampler is under vent control for which acceptable values of K_v are limited to small ranges of N_s for each value of $\frac{D}{d}$. This problem can be overcome by the use of a valve which will adjust the air vent diameter to be compatible with the existing flow conditions to ensure that the *Flow Control Number* N_c is always greater than 1.

The value of $\left(\frac{D}{d}\right)_c$ for a given sampler should be the same for nozzles of different diameter d as long as they have geometric similitude. This means that the flow rate into a sampler, having known performance characteristics, can be increased by increasing the nozzle diameter while maintaining sampler performance constant.

For all four nozzle sizes tested, values of the *Sampler Performance Coefficient* decreased as the *Sampler Number* increased with the rate of change decreasing. When the 3.18 mm (1/8") nozzle was used, values of K_n were always greater than 1.0 for all values of $\frac{D}{d}$ and therefore this size of nozzle is not a good choice for the DH-81 sampler. The 4.76 mm (3/16") nozzle should give the best results when $N_s \geq 270$ and when $\frac{D}{d} = 0.630$ implying an air vent diameter of 3 mm which is normal for the DH-81

sampler. Under these conditions values of K_n are within ±10% of the ideal value of 1.0. In the case of the 6.35 mm (1/4") nozzle, K_v increases as $\frac{D}{d}$ increases for all values of N_s, with the rate of change increasing as N_s decreases. The best results are obtained for $\frac{D}{d}$=0.393 which is equivalent to $D = 2.50$ mm. The ratio $\frac{D}{d}$ has the greatest effect on the sampler performance when the 7.94 mm (5/16") nozzle was used, having the greatest effect at the smallest value of N_s tested. The best performance with this nozzle occurs when $\frac{D}{d} = 0.251$, which is equivalent to an air vent diameter of 2.0 mm.

ACKNOWLEDGEMENT

The writers are grateful to Dr. B.G. Krishnappan and Dr. M.G. Skafel for their careful review of the manuscript and their constructive comments. The assistance provided by B. Near during the tests is much appreciated.

REFERENCES

Beverage, J.P. and J.C. Futrell, 1986. Comparison of Flume and Towing Methods for Verifying the Calibration of a Suspended Sediment Sampler. Water Resources Investigation Report 86-4193, USGS.

Cashman, M.A., 1988. Sediment Survey Equipment Catalogue. Sediment Survey Section, Water Survey of Canda Division, Water Resources Branch, Ottawa, Ontario.

Engel, P., 1989. Preliminary Examination of the Variability in the Towing Carriage Speed. NWRI Contribution 89-89, National Water Research Institute, Canada Centre for Inland Waters, Burlington, Ontario, Canada.

Engel, P. and I.G. Droppo, 1990. Preliminary Tests for the Iso-Kinetic Calibration of the DH-81 Suspended Sediment Sampler. NWRI Contribution 90-143, National Water Research Institute, Canada Centre for Inland Waters, Burlington, Ontario, Canada.

Engel, P., 1991(a). Variability in the Velocity Coefficient of Suspended Sediment Sampler Nozzles. NWRI Contribution 91-109, National Water Research Institute, Canada Centre for Inland Waters, Burlington, Ontario, Canada.

Engel, P., 1991(b). Basic Requirements for Iso-Kinetic Operations of Large Volume Point Integrating Sediment Samplers. NWRI Contribution 91-120, National Water Research Institute, Canda Centre for Inland Waters, Burlington, Ontario, Canada.

Guy, H.P. and V.W. Norman, 1970. Field Methods for Measurement of Fluvial Sediment. Techniques of Water Resources Investigations of the United States Geological Survey, United States Government Printing Office, Washington, D.C.

Skinner, J., 1979. Operating Instructions; D - 77 Suspended Sediment Sampler. Federal Inter-Agency Sedimentation Project, St. Anthony Falls Hydraulics Laboratory, Minneapolis, Minnesota, USA.

T.C.P.S.M., 1969. Sediment Measurement Techniques: A. Fluvial Sediment. Task Committee on Preparation of Sedimentation Manual, Committee on Sedimentation of the Hydraulics Division, Journal of the Hydraulics Division, Proceedings of the American Society of Civil Engineers, Vo. 95, No. HY5, pp 1477-1543.

U.S. Army Corps of Engineers, 1941. Laboratory Investigation of Suspended Sediment Samplers, Report No.5, St. Paul U.S. District Sub-Office, Hydraulics Laboratory, University of Iowa, Iowa City, Iowa.

TABLE 1
Test Data for the DH-81 Sampler
with 3.18 mm (1/8") Nozzle

V_c $[m/s]$	Q_s $[cm^3/s]$	V_n $[m/s]$	D $[mm]$
0.20	-	-	1.0
0.40	2.7	0.341	1.0
0.60	4.3	0.543	1.0
0.80	6.5	0.821	1.0
1.00	9.0	1.136	1.0
0.20	-	-	1.5
0.40	4.4	0.556	1.5
0.60	5.7	0.720	1.5
0.80	7.5	0.947	1.5
1.00	9.7	1.225	1.5
0.20	3.4	0.429	2.0
0.40	4.9	0.619	2.0
0.60	6.5	0.821	2.0
0.80	8.5	1.073	2.0
1.00	10.4	1.313	2.0
0.20	3.2	0.404	2.5
0.40	4.3	0.543	2.5
0.60	6.1	0.770	2.5
0.80	8.3	1.048	2.5
1.00	10.7	1.351	2.5
0.20	4.2	0.530	3.0
0.40	5.5	0.694	3.0
0.60	7.0	0.884	3.0
0.80	8.2	1.035	3.0
1.00	10.7	1.351	3.0

TABLE 2
Test Data for the DH-81 Sampler
with 4.76 mm (3/16") Nozzle

V_c $[m/s]$	Q_s $[cm^3/s]$	V_n $[m/s]$	D $[mm]$
0.20	-	-	1.0
0.40	5.0	0.281	1.0
0.60	7.3	0.410	1.0
0.80	10.3	0.579	1.0
1.00	13.8	0.775	1.0
0.20	-	-	1.5
0.40	9.0	0.506	1.5
0.60	10.7	0.601	1.5
0.80	13.2	0.742	1.5
1.00	16.1	0.905	1.5
0.20	5.8	0.326	2.0
0.40	8.0	0.449	2.0
0.60	10.7	0.601	2.0
0.80	13.5	0.758	2.0
1.00	16.7	0.938	2.0
0.20	6.9	0.388	2.5
0.40	8.7	0.489	2.5
0.60	11.3	0.635	2.5
0.80	14.3	0.803	2.5
1.00	17.7	0.994	2.5
0.20	7.0	0.393	3.0
0.40	8.9	0.500	3.0
0.60	11.4	0.640	3.0
0.80	14.3	0.803	3.0
1.00	17.7	0.994	3.0

TABLE 3
Test Data for the DH-81 Sampler
with 6.35 mm (1/4") Nozzle

V_c $[m/s]$	Q_s $[cm^3/s]$	V_n $[m/s]$	D $[mm]$
0.20	-	-	1.0
0.40	9.2	0.290	1.0
0.60	11.2	0.354	1.0
0.80	13.8	0.436	1.0
1.00	17.3	0.546	1.0
0.20	-	-	1.5
0.40	12.5	0.395	1.5
0.60	15.8	0.499	1.5
0.80	20.0	0.632	1.5
1.00	25.0	0.789	1.5
0.20	11.2	0.354	2.0
0.40	14.3	0.452	2.0
0.60	18.2	0.575	2.0
0.80	22.5	0.711	2.0
1.00	27.5	0.868	2.0
0.20	10.9	0.344	2.5
0.40	14.1	0.445	2.5
0.60	18.5	0.584	2.5
0.80	23.3	0.736	2.5
1.00	29.0	0.916	2.5
0.20	13.4	0.423	3.0
0.40	16.0	0.505	3.0
0.60	19.8	0.625	3.0
0.80	24.5	0.774	3.0
1.00	30.3	0.957	3.0

TABLE 4
Test Data for the DH-81 Sampler
with 7.94 mm (5/16") Nozzle

V_c $[m/s]$	Q_s $[cm^3/s]$	V_n $[m/s]$	D $[mm]$
0.20	-	-	1.0
0.40	10.8	0.218	1.0
0.60	13.0	0.263	1.0
0.80	16.2	0.327	1.0
1.00	20.2	0.408	1.0
0.20	15.5	0.313	1.5
0.40	17.1	0.345	1.5
0.60	21.4	0.432	1.5
0.80	27.3	0.551	1.5
1.00	34.8	0.703	1.5
0.20	17.7	0.358	2.0
0.40	23.3	0.471	2.0
0.60	29.5	0.596	2.0
0.80	36.7	0.741	2.0
1.00	43.9	0.887	2.0
0.20	20.8	0.420	2.5
0.40	26.0	0.525	2.5
0.60	32.7	0.661	2.5
0.80	40.1	0.810	2.5
1.00	48.5	0.980	2.5
0.20	24.6	0.497	3.0
0.40	29.8	0.602	3.0
0.60	36.4	0.735	3.0
0.80	43.7	0.883	3.0
1.00	52.0	1.050	3.0

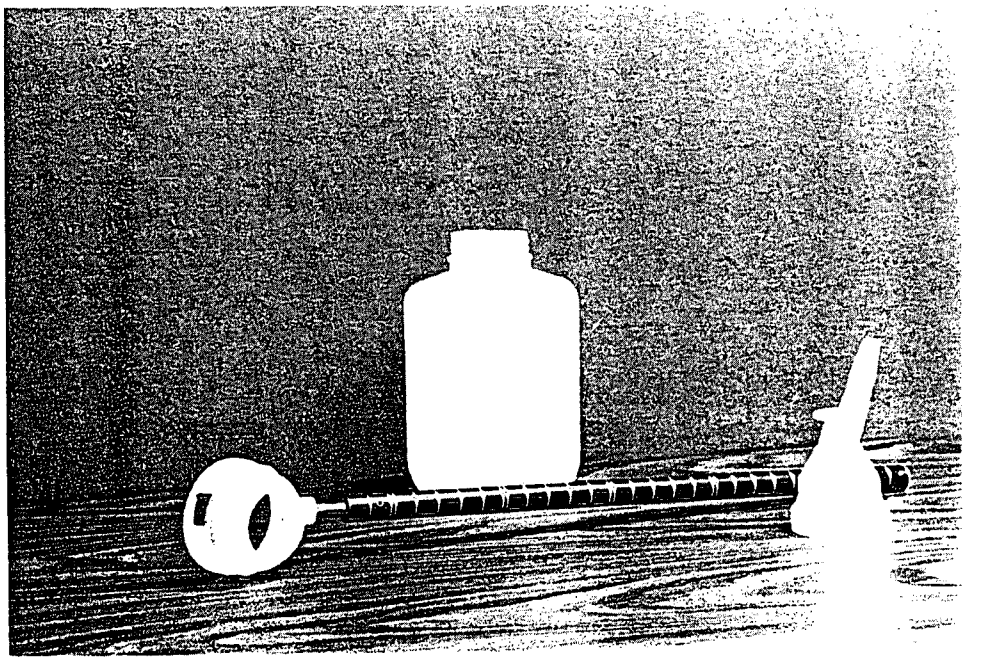

Figure 1. Components of USDH-81 sampler

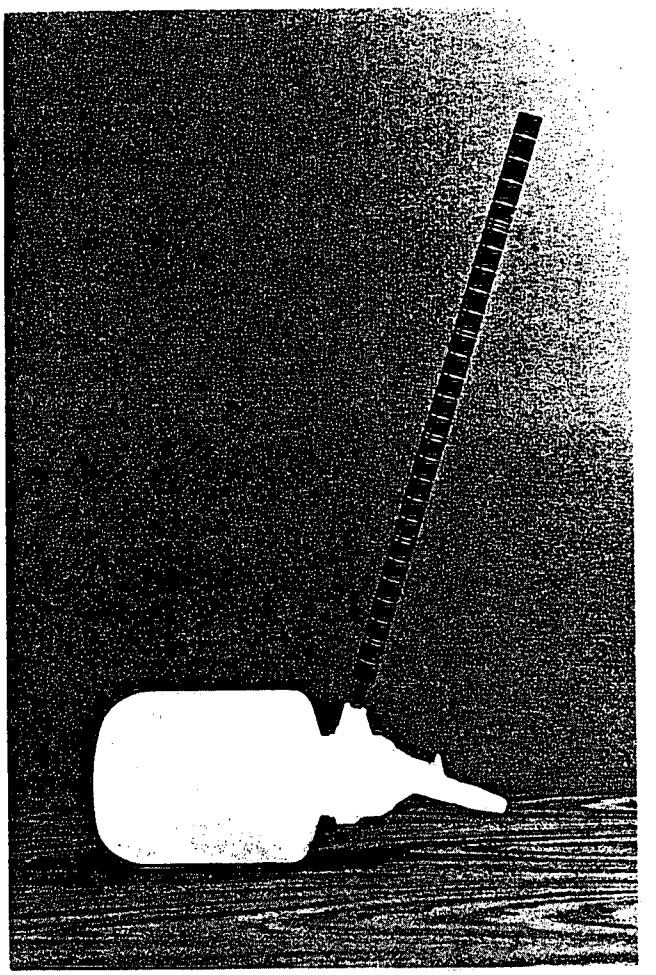

Figure 2. USDH-81 sampler assembled

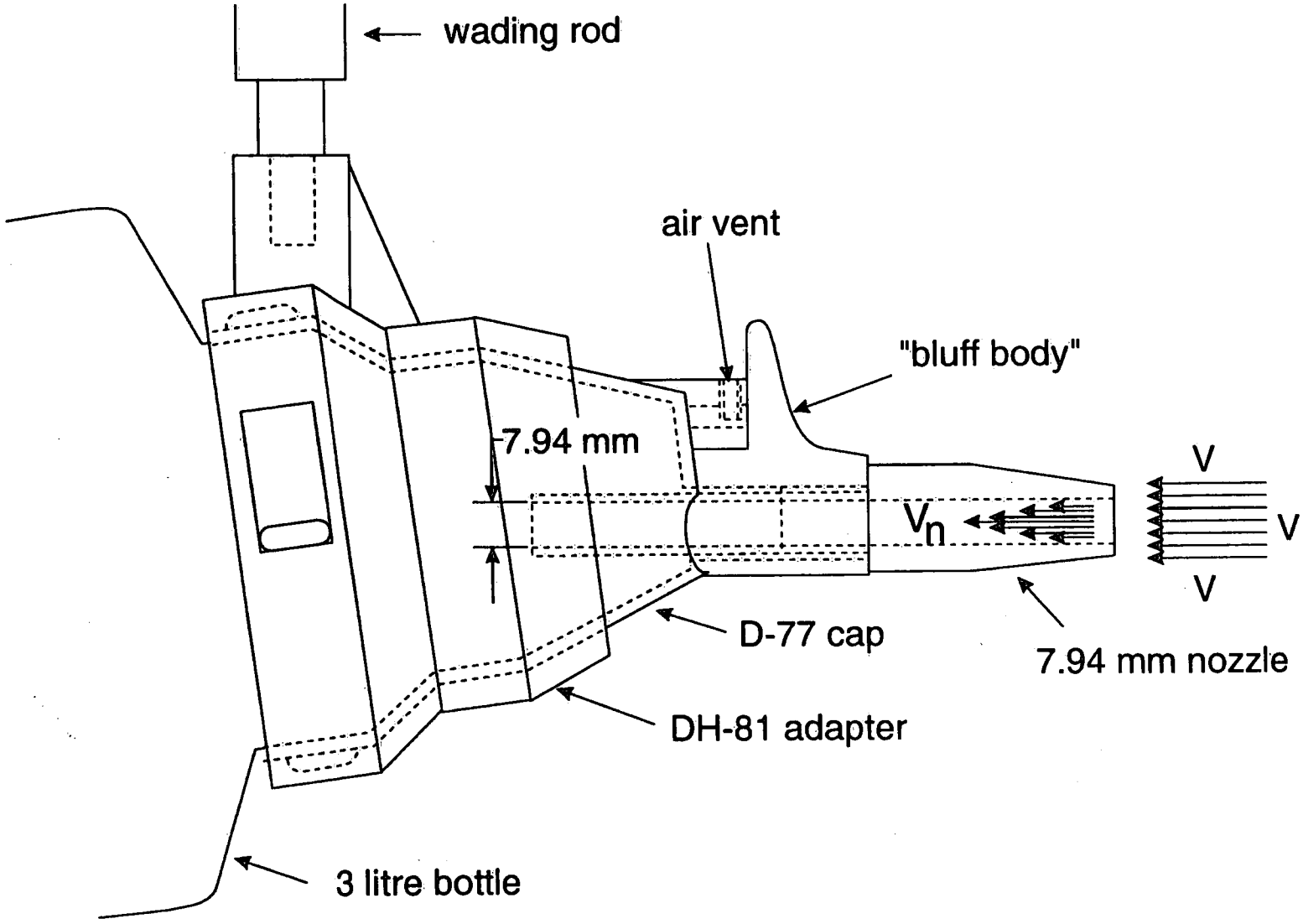

Figure 3 DH - 81 sampler cap detail with 7.94 mm nozzle.

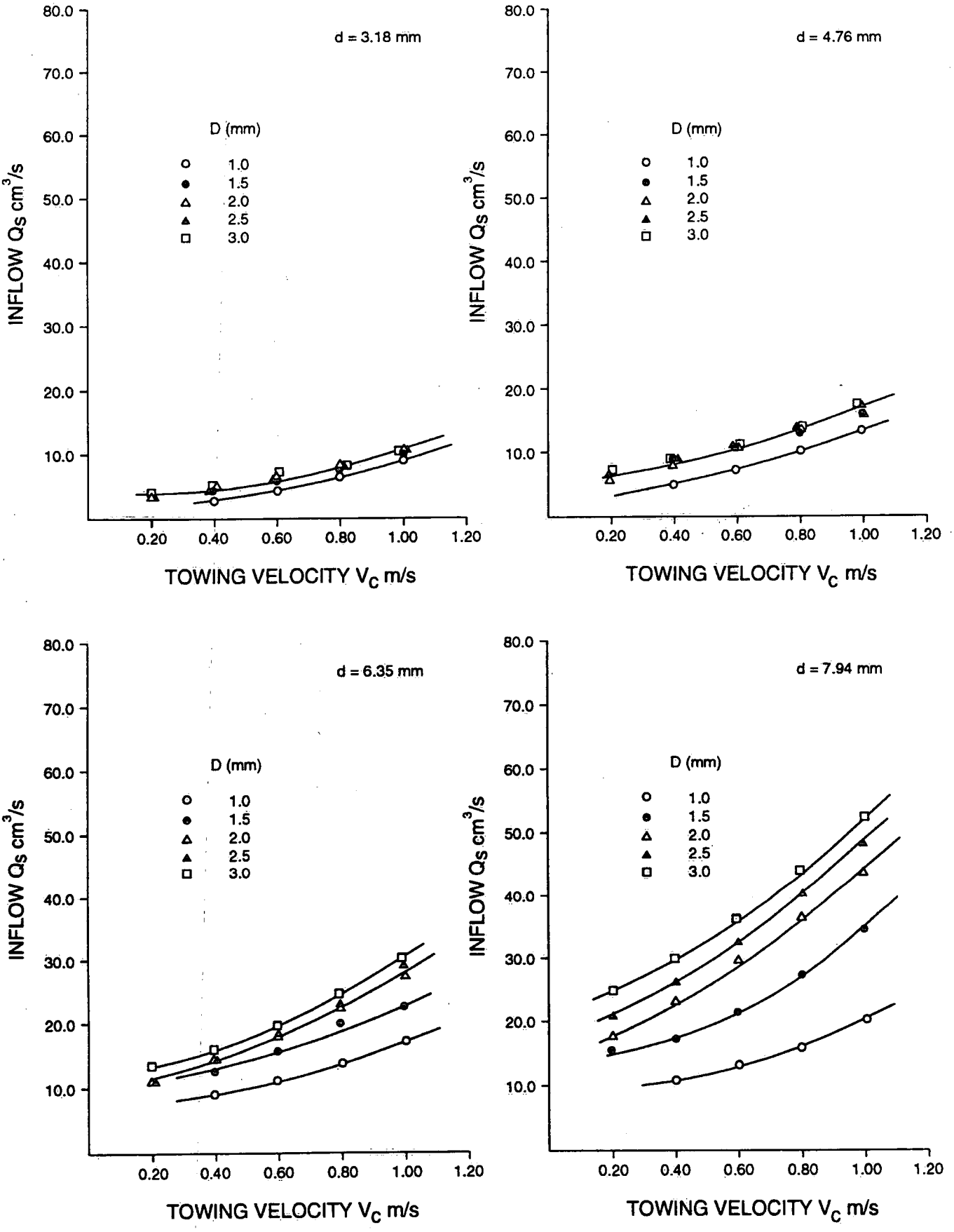

Figure 4 Flow into sampler as a function of towing velocity with vent diameter as a parameter.

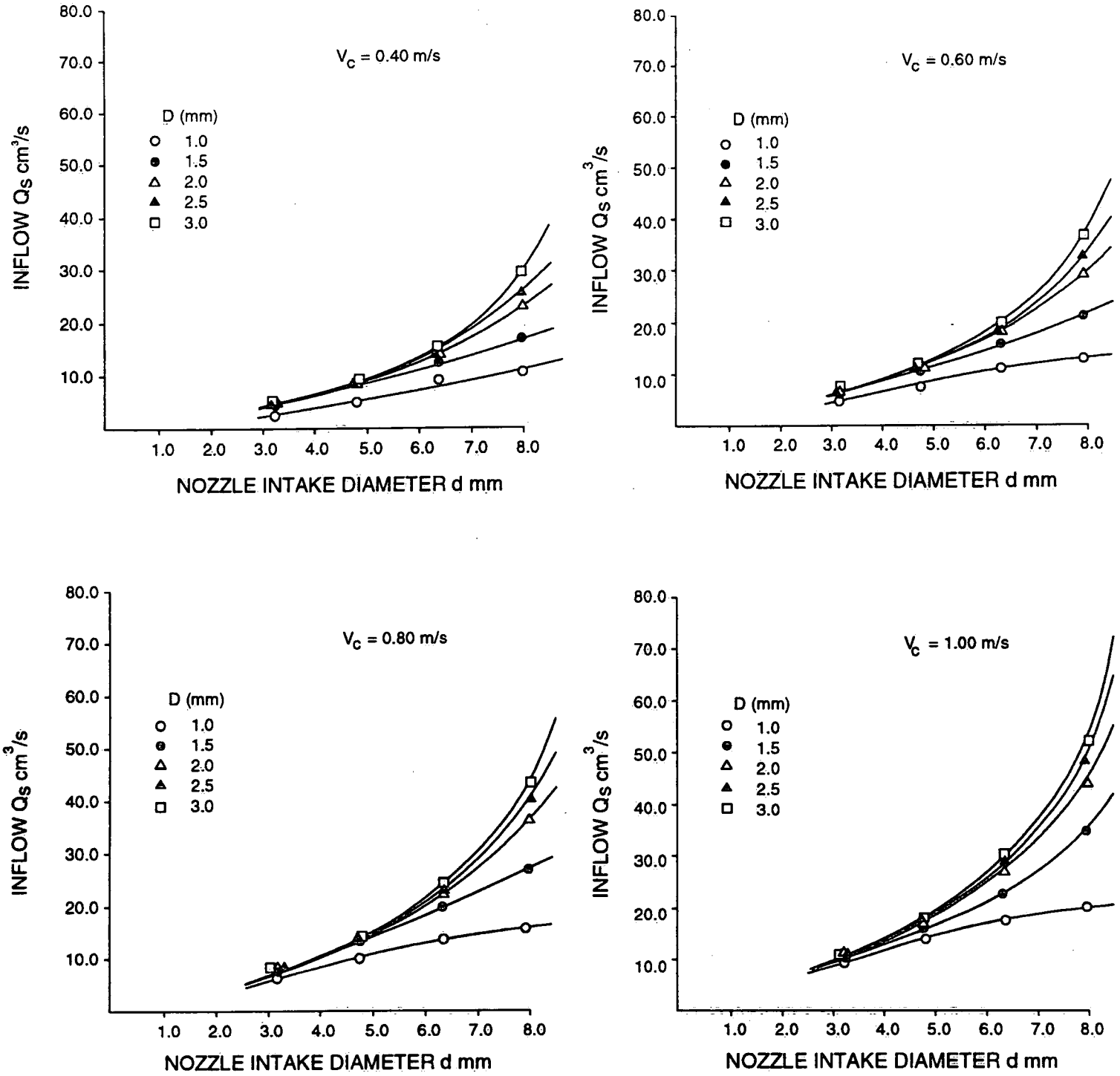

Figure 5 Flow into the sampler as a function of nozzle diameter with vent diameter as a parameter.

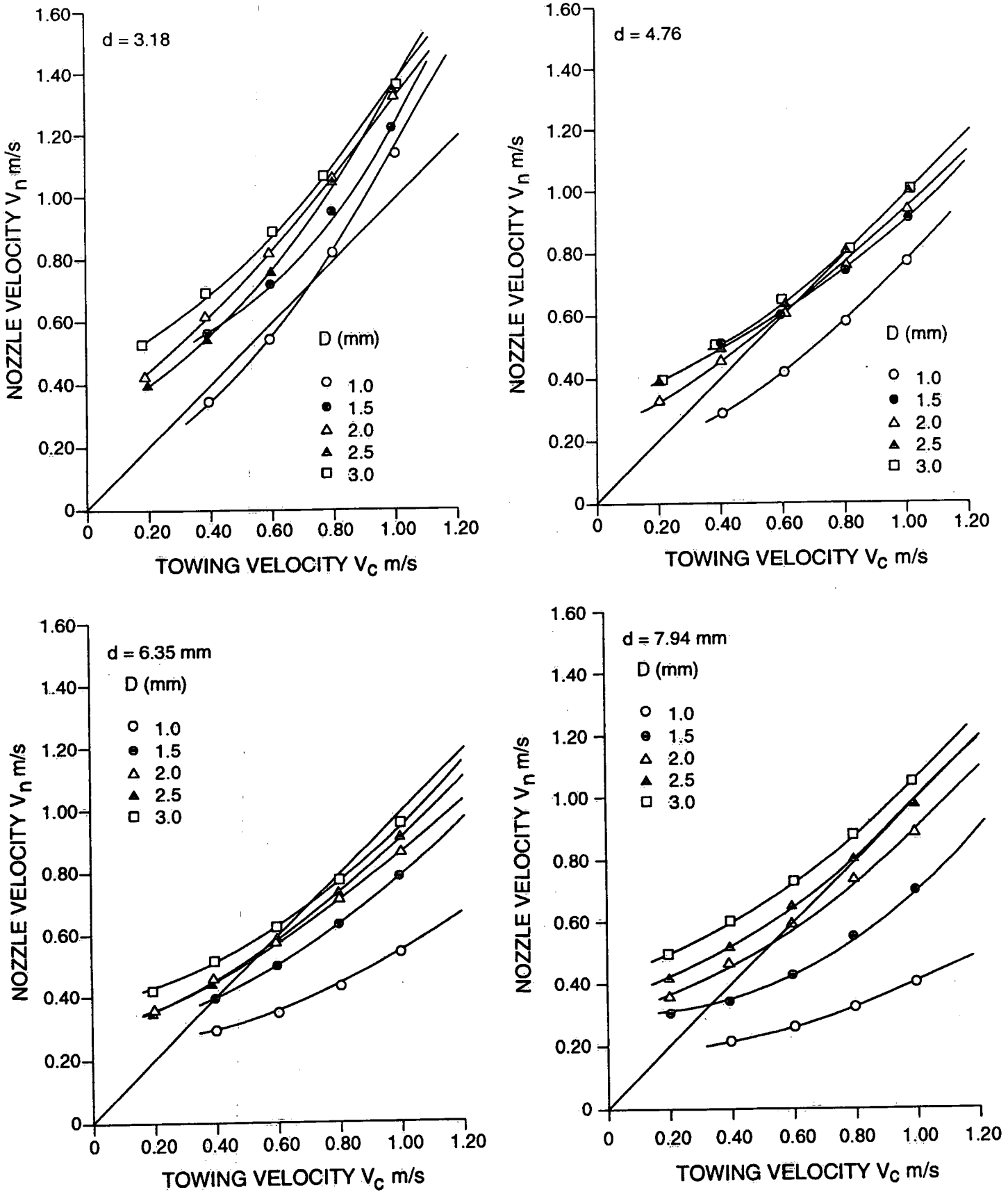

Figure 6 Nozzle velocity as a function of towing velocity with D as a parameter

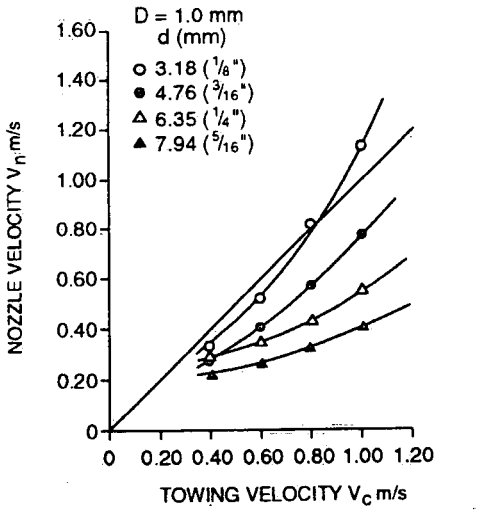

Effect of nozzle size when D = 1.0 mm

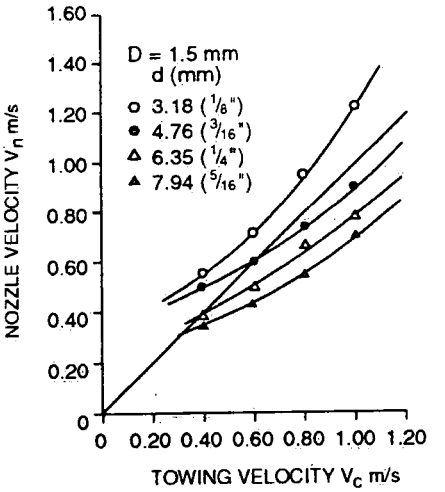

Effect of nozzle size when D = 1.5 mm

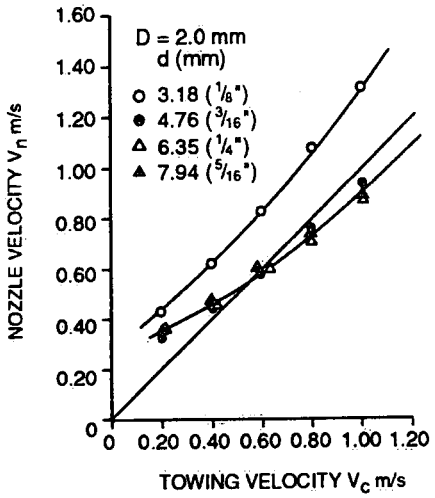

Effect of nozzle size when D = 2.0 mm

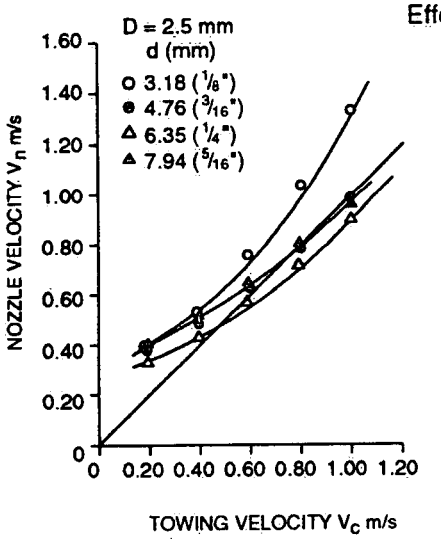

Effect of nozzle size when D = 2.5

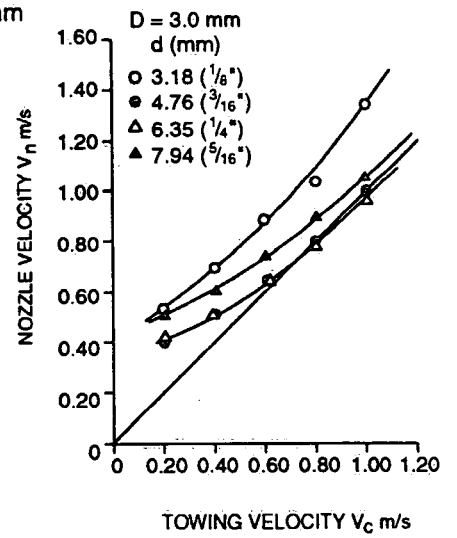

Effect of nozzle size when D = 3.0

Figure 7 Nozzle velocity as a function of towing velocity with d as a parameter

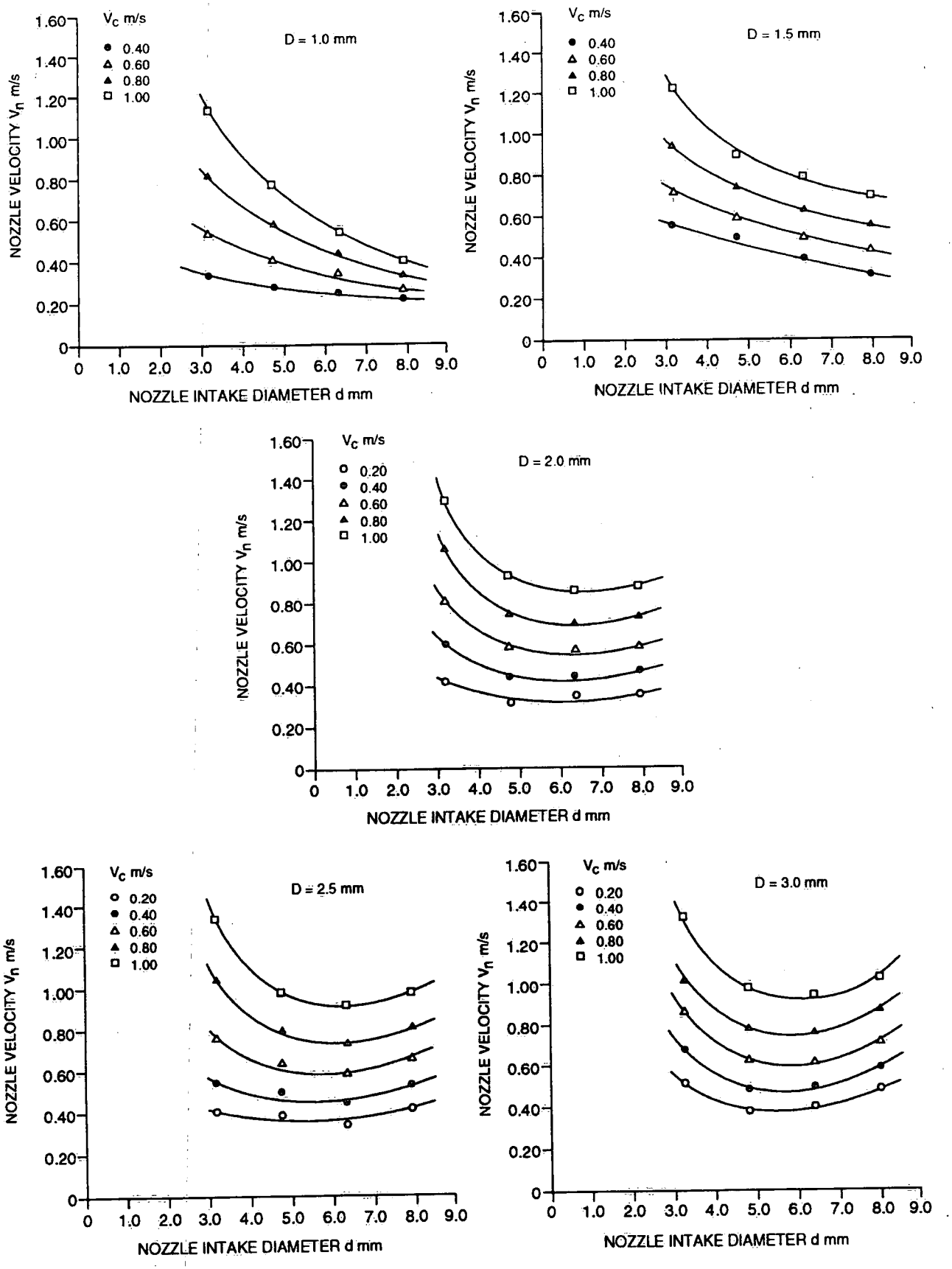

Figure 8 Nozzle velocity as a function of nozzle diameter with V_c as a parameter

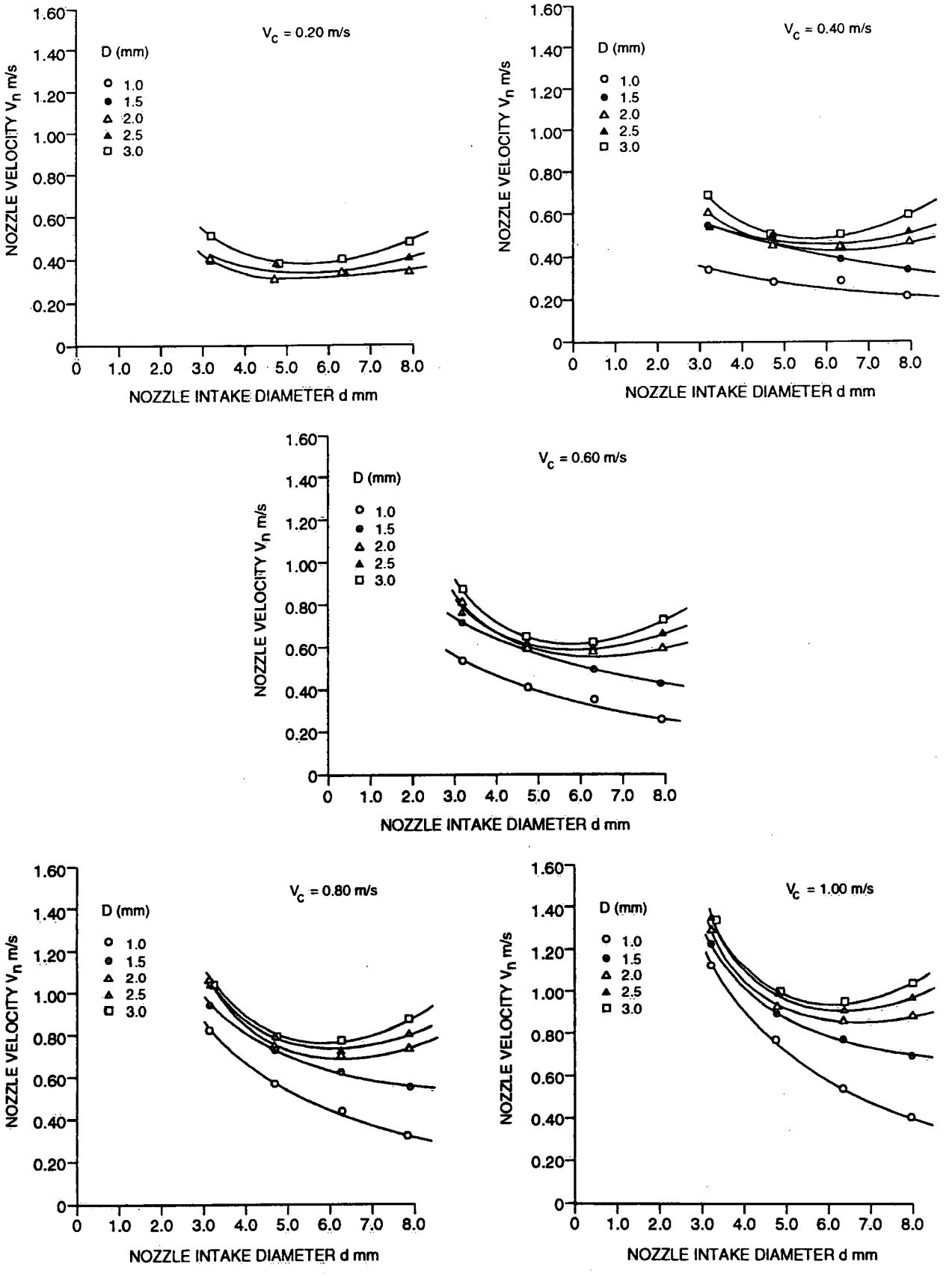

Figure 9 Nozzle velocity as a function of nozzle diameter with D as a parameter.

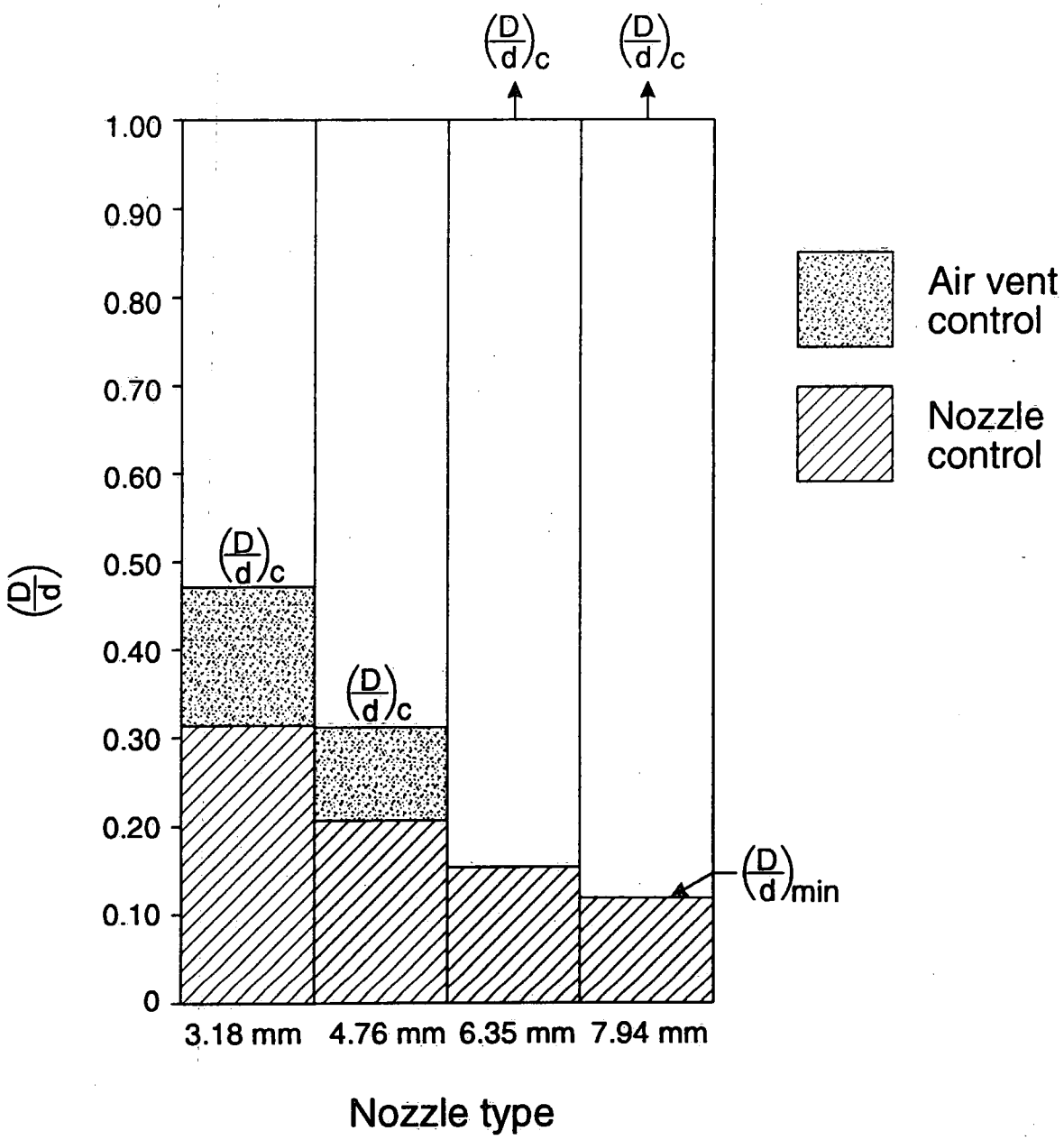

Figure 10 Flow control diagram.

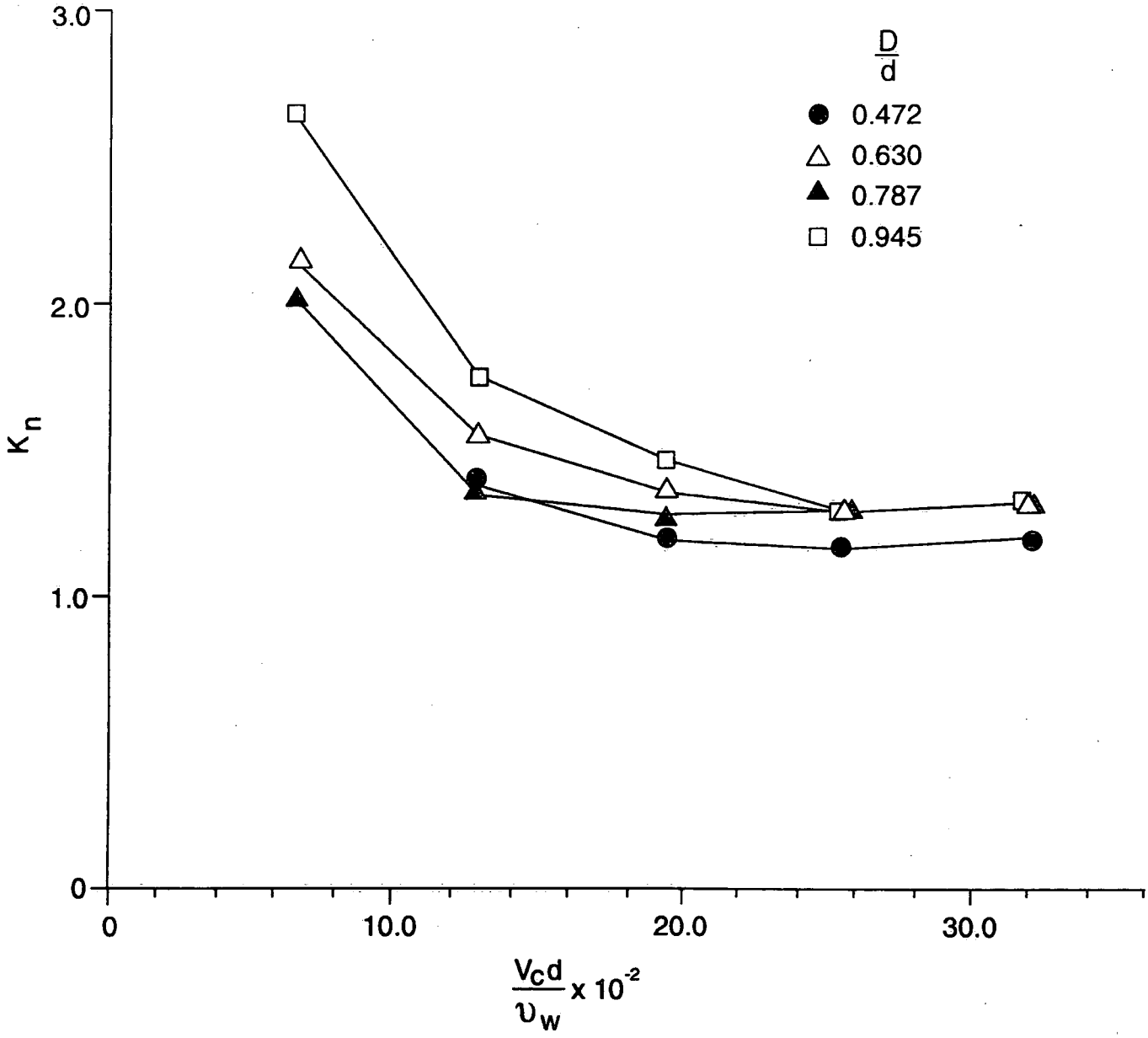

Figure 11 Performance coefficient under nozzle control with 3.18 mm nozzle.

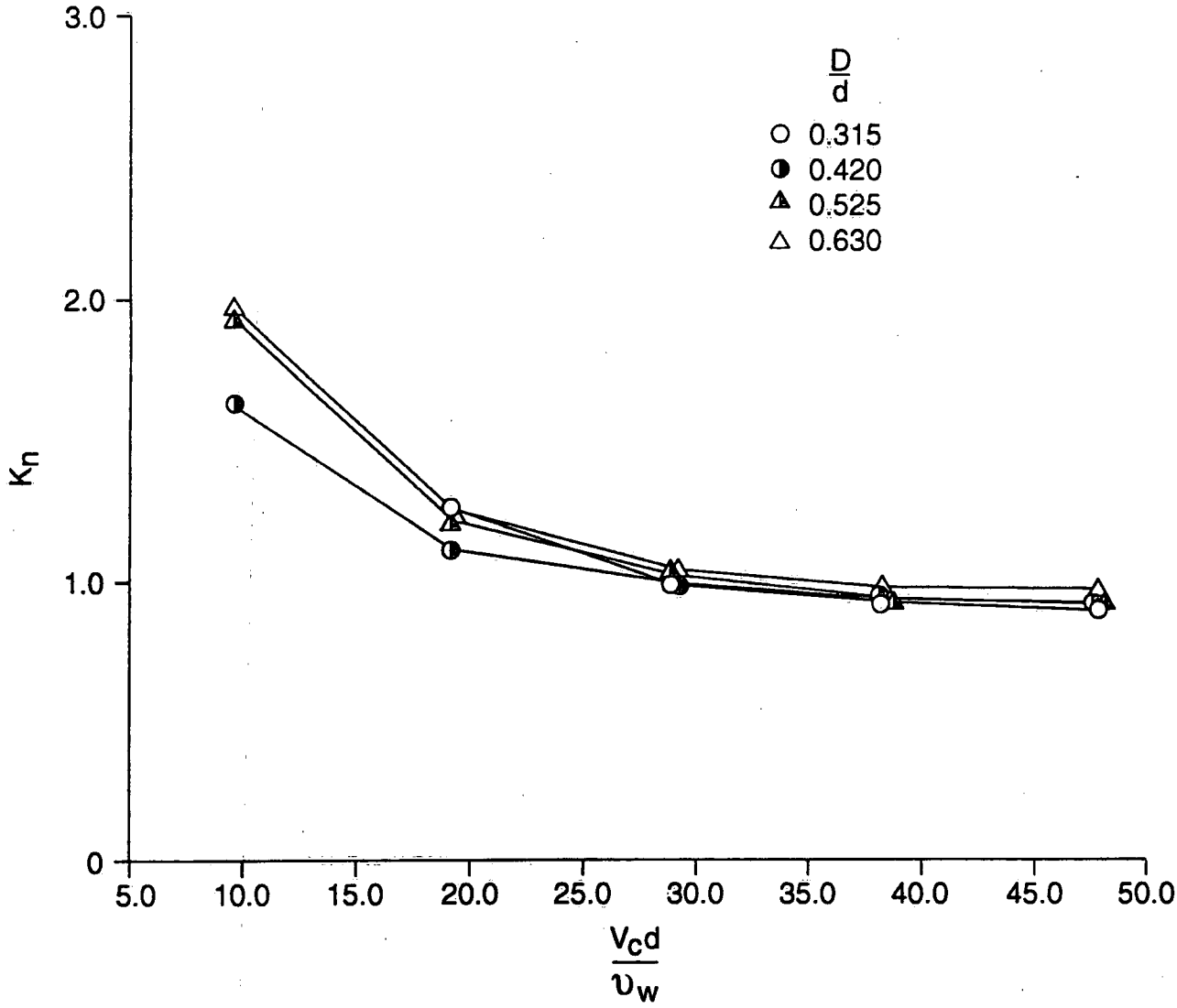

Figure 12 Performance coefficient under nozzle control with 4.76 mm nozzle

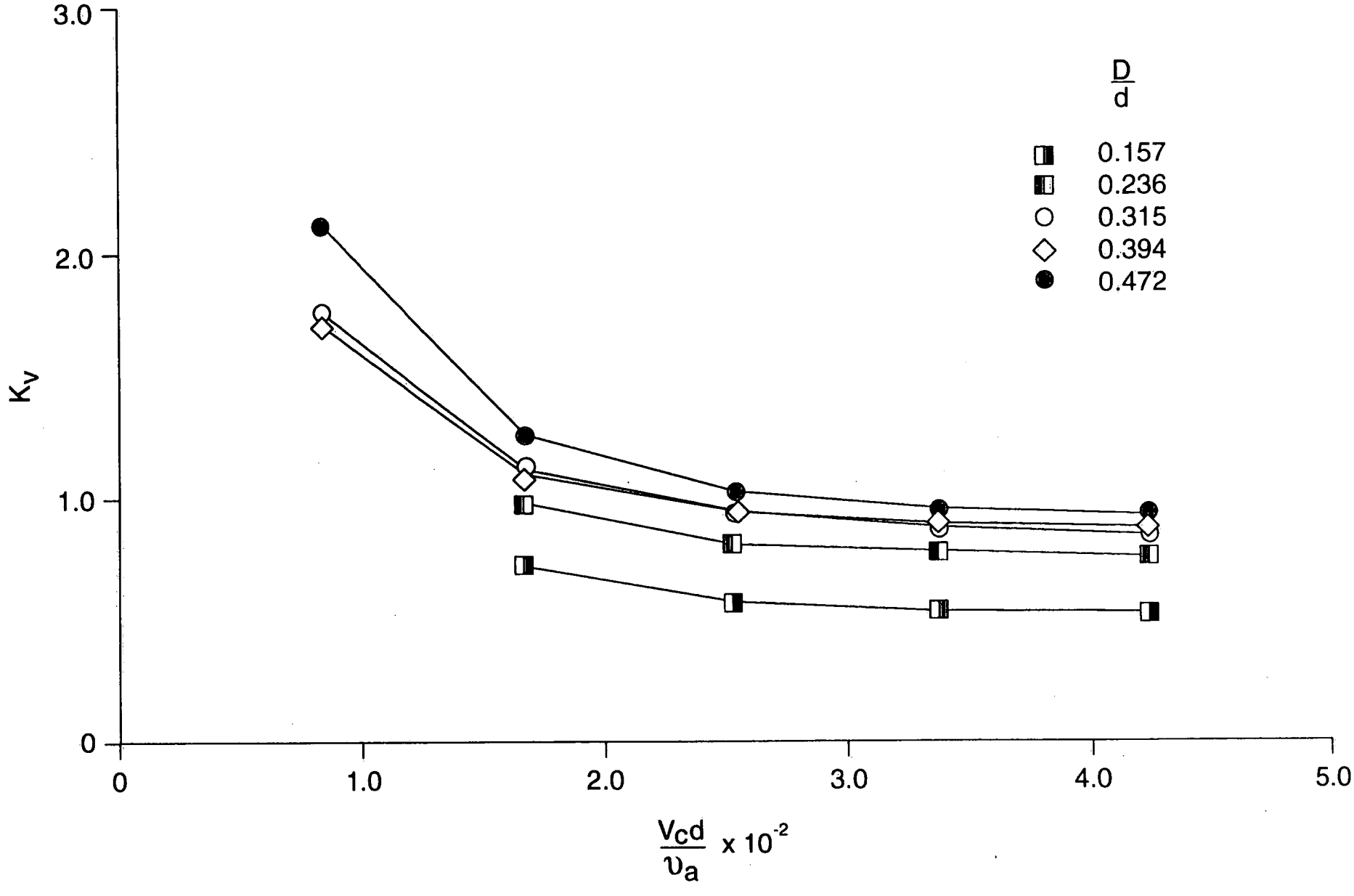

Figure 13 Performance coefficient under vent control with 6.35 mm nozzle

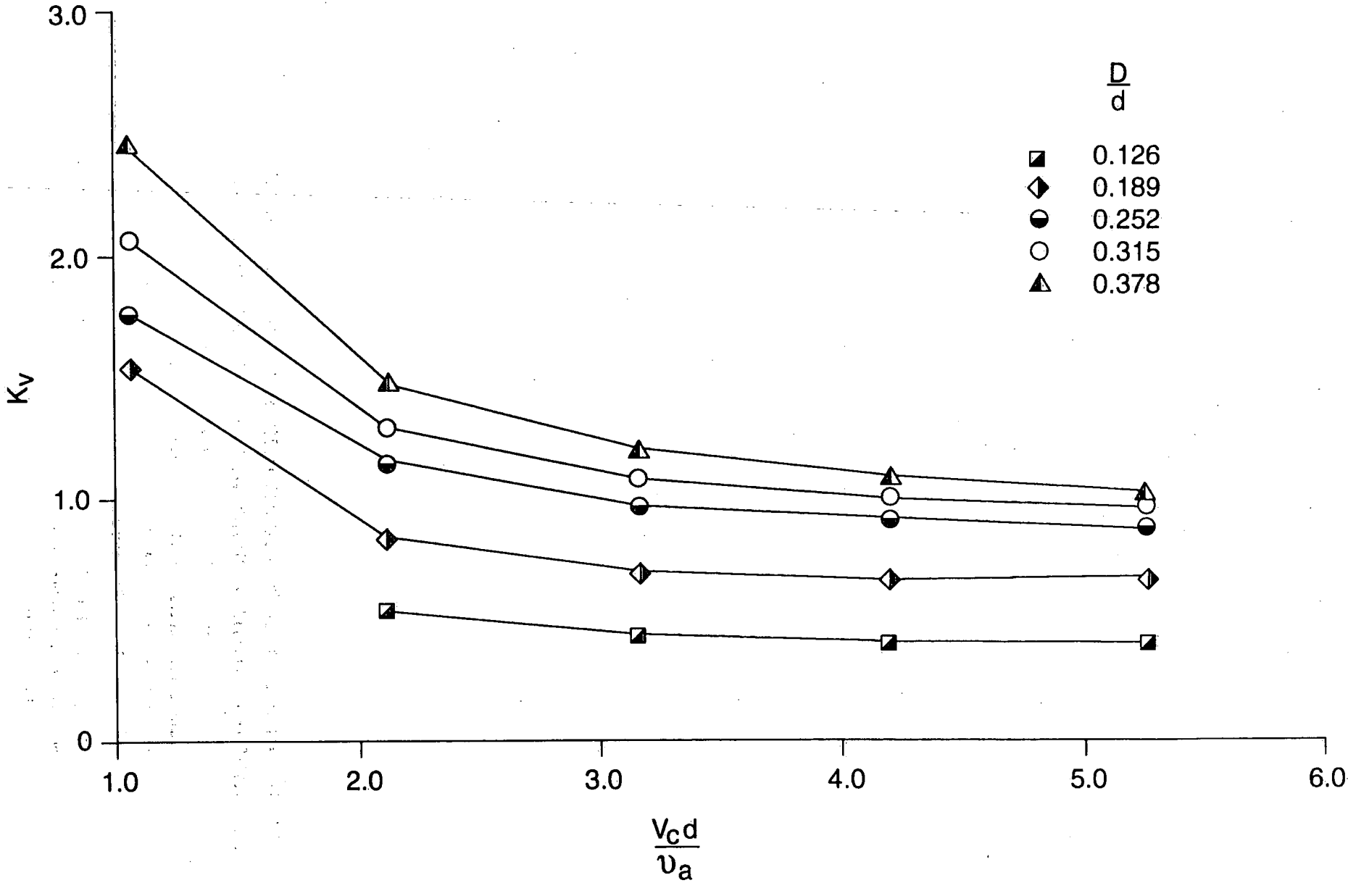

Figure 14 Performance coefficient under vent control with 7.94 mm nozzle

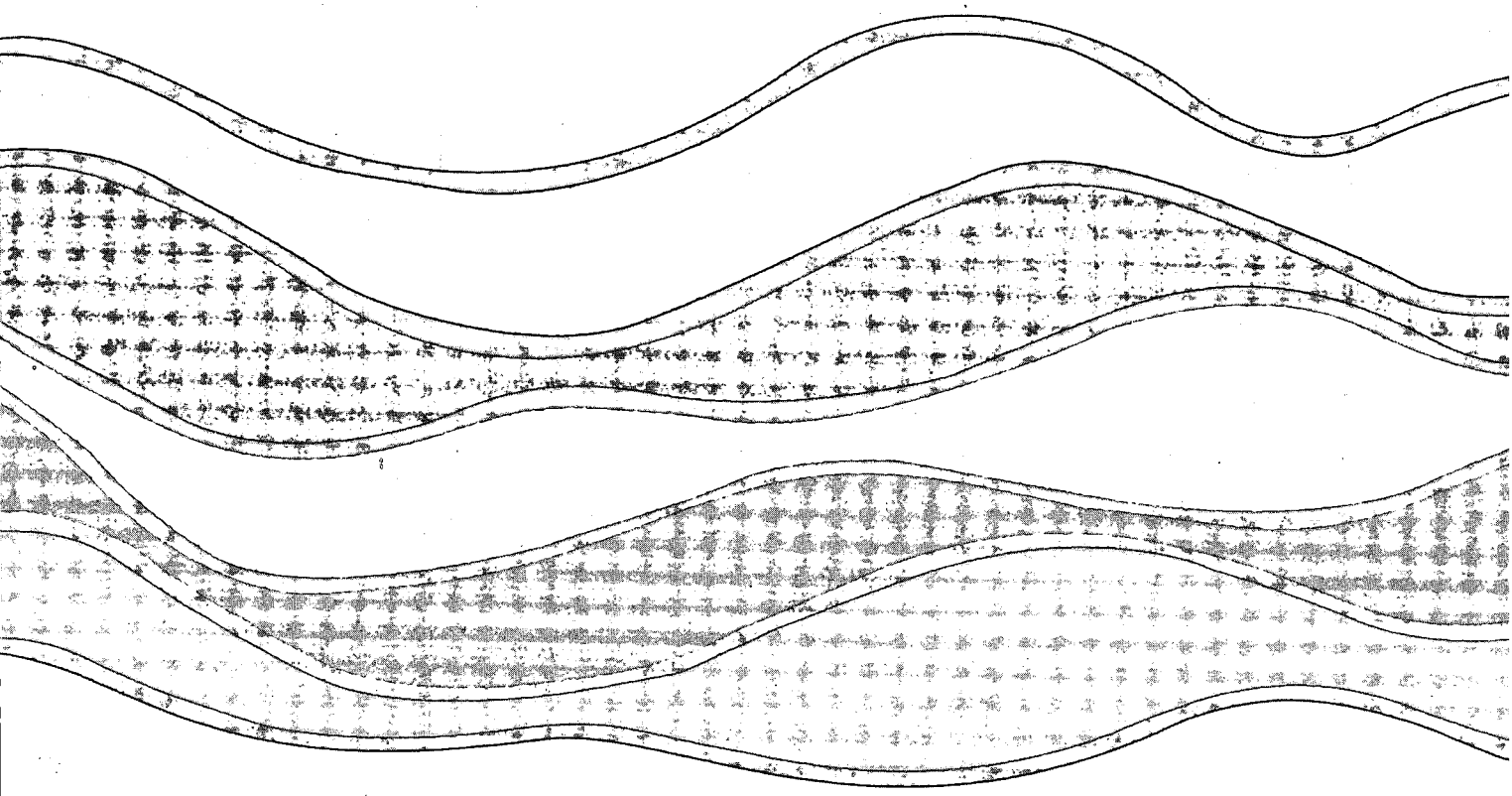

NATIONAL WATER RESEARCH INSTITUTE
P.O. BOX 5050, BURLINGTON, ONTARIO L7R 4A6

Environment Canada Environnement Canada

Canada

INSTITUT NATIONAL DE RECHERCHE SUR LES EAUX
C.P. 5050, BURLINGTON (ONTARIO) L7R 4A6

Think Recycling!

Pensez à Recycling!